

Radical-Anionic Cyclizations of Eneidyne: Remarkable Effects of Benzannelation and Remote Substituents on Cycloaromatization Reactions

Igor V. Alabugin* and Mariappan Manoharan

Contribution from the Department of Chemistry and Biochemistry, Florida State University, Tallahassee, Florida 32306-4390

Received December 10, 2002; E-mail: alabugin@chem.fsu.edu

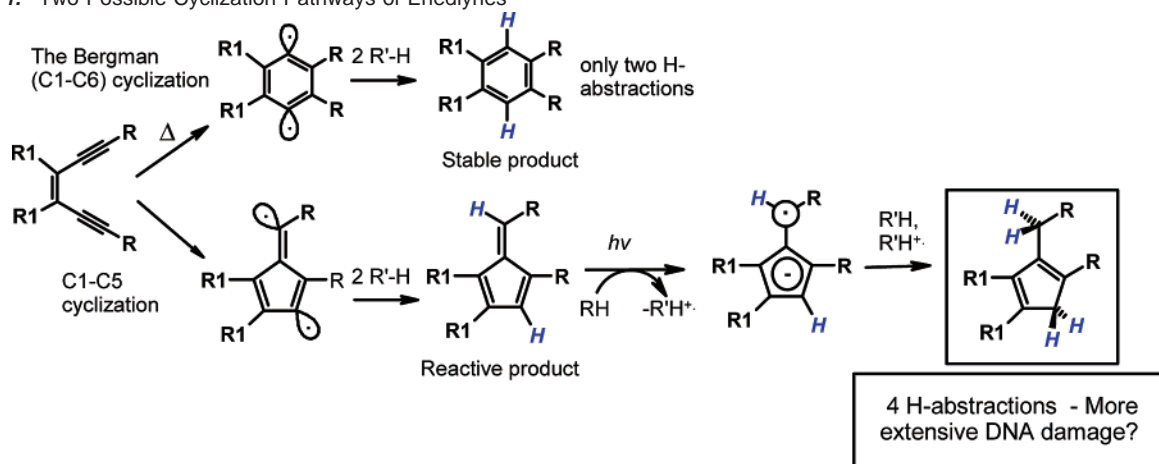
Abstract: The reasons for large changes in the energetics of C1–C5 and C1–C6 (Bergman) cyclizations of eneidyne upon one-electron reduction were studied by DFT and Coupled Cluster computations. Although both of these radical-anionic cyclizations are significantly accelerated relative to their thermal counterparts, the acceleration is especially large for *benzannelated* eneidyne, whose reductive cyclizations are predicted to proceed readily under ambient conditions. Unlike their thermal analogues, the radical-anionic reactions can be efficiently controlled by remote substitution, and the effect of substituent electronegativity is *opposite* of the effect on the thermal cycloaromatization reactions. For both radical-anionic cyclizations, large effects of benzannelation and increased sensitivity to the properties of remote substituents result from crossing of *out-of-plane* and *in-plane* MOs in the vicinity of transition states. This crossing leads to restoration of the aromaticity decreased upon one-electron reduction of benzannelated eneidyne. Increased interactions between nonbonding orbitals as well as formation of new aromatic rings (five membered for the C1–C5 cyclization and six membered for C1–C6 cyclizations) are the other sources of increased exothermicity for both radical-anionic cyclizations. The tradeoff between reduction potentials and cyclization efficiency as well as the possibilities of switching of eneidyne cyclization modes (*exo* or C1–C5 vs *endo* or C1–C6)) under kinetic or thermodynamic control conditions are also outlined.

Introduction

Cycloaromatization reactions,¹ especially the well-known cyclization of (*Z*)-3-ene-1,5-diyne to 1,4-benzene σ,σ -diradicals (*p*-benzynes) (the Bergman cyclization)² have found a number of practical applications, such as in the development of anticancer drugs,³ in the design of sequence-specific DNA cleavage and mapping tools,⁴ in the pursuit of polymeric materials with improved thermal stability,⁵ and in the synthesis of polycyclic compounds.⁶ Success of these applications depends on control over eneidyne reactivity through either strain^{7–10} or electronic effects.^{11–14} Unfortunately, because the developing

radical centers are orthogonal to the aromatic π -system,^{15,16} neither benzannelation itself nor the nature of para substituents

- (1) For representative examples of a variety of cycloaromatization reactions, see: (a) Nagata, R.; Yamanaka, H.; Okazaki, E.; Saito, I. *Tetrahedron Lett.* **1989**, *30*, 4995. Myers, A. G.; Dragovich, P. S.; Kuo, E. Y. *J. Am. Chem. Soc.* **1992**, *114*, 9369. (b) Nakatani, K. Isoe, S.; Maekawa, S. Saito, I. *Tetrahedron Lett.* **1994**, *35*, 605. Sullivan, R. W.; Coghlan, V. M.; Munk, S. A.; Reed, M. W.; Moore, H. W. *J. Org. Chem.* **1994**, *59*, 2276. (c) Toda, F.; Tanaka, K.; Sano, I.; Isozaki, T. *Angew. Chem., Int. Ed. Engl.* **1994**, *33*, 1757. (d) Nicolaou, K. C.; Skokotas, G.; Maligres, P.; Zuccarello, G.; Schweiger, E. J.; Toshima, K.; Wendeborn, S. *Angew. Chem., Int. Ed. Engl.* **1989**, *28*, 1272. (e) Engels, B.; Lennartz, C.; Hanrath, M.; Schmittel, M.; Strittmatter, M. *Angew. Chem., Int. Ed. Engl.* **1998**, *37*, 2067. (f) Schmittel, M.; Steffen, J.-P.; Angel, M. A. W.; Engels, B.; Lennartz, C.; Hanrath, M. *Angew. Chem., Int. Ed.* **1998**, *37*, 2067. (g) Schmittel, M.; Rodriguez, D.; Steffen, J. P. *Angew. Chem., Int. Ed.* **2000**, *39*, 2067. (h) Kawatkar, S. P.; Schreiner, P. R. *Org. Lett.*, **2002**, *4*, 3643.
- (2) Jones, R. R.; Bergman, R. G. *J. Am. Chem. Soc.* **1972**, *94*, 660. Bergman, R. G. *Acc. Chem. Res.* **1973**, *6*, 25–31.
- (3) (a) *Eneidyne Antibiotics as Antitumor Agents*; Borders, D. B., Doyle, T. W., Eds.; Marcel Dekker: New York, 1995. (b) *Neocarzinostatin: The Past, Present, and Future of an Anticancer Drug*; Maeda, H., Edo, K., Ishida, N., Eds.; Springer: New York, 1997.
- (4) Wu, M.; Stoermer, D.; Tullius, T.; Townsend, C. A. *J. Am. Chem. Soc.* **2000**, *122*, 12884.
- (5) Chen, X.; Tolbert, L. M.; Hess, D. W.; Henderson, C. *Macromolecules* **2001**, *34*, 4104. Shah, H. V.; Babb, D. A.; Smith, Jr., D. W. *Polymer* **2000**, *41*, 4415. John, J. A.; Tour, J. M. *J. Am. Chem. Soc.* **1994**, *116*, 5011.
- (6) The Bergman reaction as a synthetic tool: Bowles, D. M.; Palmer, G. J.; Landis, C. A.; Scott, J. L.; Anthony, J. E. *Tetrahedron* **2001**, *57*, 3753. Bowles, D. M.; Anthony, J. E. *Org. Lett.* **2000**, *2*, 85.
- (7) Incorporation of the eneidyne unit into a strained 9- or 10-membered ring was shown to facilitate the reaction through ground-state destabilization. For selected experimental work, see: (a) Nicolaou, K. C.; Zuccarello, G.; Ogawa, Y.; Schweiger, E. J.; Kumazawa, T. *J. Am. Chem. Soc.* **1988**, *110*, 4866. (b) Nicolaou, K. C.; Zuccarello, G.; Riemer, C.; Estevez, V. A.; Dai, W.-M. *J. Am. Chem. Soc.* **1992**, *114*, 7360. (c) Iida, K.; Hiram, M. *J. Am. Chem. Soc.* **1995**, *117*, 8875.
- (8) Snyder, J. P. *J. Am. Chem. Soc.* **1989**, *111*, 7630. Snyder, J. P.; Tipword, G. E. *J. Am. Chem. Soc.* **1990**, *112*, 4040. Snyder, J. P. *J. Am. Chem. Soc.* **1990**, *112*, 5367.
- (9) (a) Kraka, E.; Cremer, D. *J. Am. Chem. Soc.* **1994**, *116*, 4929. (b) Schreiner, P. R., in ref 26. (c) Alabugin, I. V.; Manoharan, M. *J. Phys. Chem. A* **2003**, ASAP article (JP026754c, 12/18/2002).
- (10) The cyclization can also be controlled by release of strain in the transition state: Magnus, P.; Carter, P.; Elliott, J.; Lewis, R. Harling, J. Pitterna, T.; Bauta, W. E.; Fortt, S. *J. Am. Chem. Soc.* **1992**, *114*, 2544.
- (11) Schmittel, M.; Kiau, S. *Chem. Lett.* **1995**, 953–954.
- (12) Mayer, M. E.; Greiner, B. *Liebigs Ann. Chem.* **1992**, 855–861.
- (13) Choy, N.; Kim, C.-S.; Ballester, C.; Argitas, L.; Diez, C.; Lichtenberg, F.; Shapiro, J.; Russell, K. C. *Tetrahedron Lett.* **2000**, *41*, 6995. Correlation of the reaction rate with the Hammett σ_m value revealed a low sensitivity to substituents ($\rho = 0.654$). The Swain–Lupton model yielded a field parameter (0.662) larger than the resonance π parameter (0.227), indicating that conjugative effects in the out-of-plane π -system are of lesser importance than field effects.
- (14) Jones, G. B.; Plourde, G. W. *Org. Lett.* **2000**, *2*, 1757. Jones, G. B.; Warner, P. M. *J. Am. Chem. Soc.* **2001**, *123*, 2134. Plourde, G. W., II; Warner, P. M.; Parrish, D. A.; Jones, G. B. *J. Org. Chem.* **2002**, *67*, 5369–5374. Jones, G. B.; Wright, J. M.; Hynd, G.; Wyatt, J. K.; Warner, P. M.; Huber, R. S.; Li, A.; Kilgore, M. W.; Sticca, R. P.; Pollenz, R. S. *J. Org. Chem.* **2002**, *67*, 5727–5732.

Scheme 1. Two Possible Cyclization Pathways of Enediyne^a

^a Hydrogen atoms (H atoms) abstracted from the environment are shown in blue italics.

in the annealed benzene ring has a large effect on the cyclization rate.^{13,17} This complicates efficient control and rational design of cycloaromatization reactions.

An important feature of cycloaromatization reactions is the presence of two mutually perpendicular arrays of π -orbitals, which play different roles during the cyclization process. While the in-plane π -orbitals are sacrificed in order to form a σ -bond and two radical centers, the out-of-plane π -orbitals are conserved but transformed into a cyclic (usually aromatic) π -system. The different roles of these two π -systems, which are crucial for understanding and control of cycloaromatization reactions, were most clearly outlined in a recent paper of Schreiner, Shaik, and co-workers, who applied valence bond (VB) theory to analyze the relative timing of changes in the *in-plane* and *out-of-plane* systems during the Bergman cyclization of parent enediyne **3**.¹⁶ In short, the changes in the in-plane orbitals were found to occur much earlier along the reaction path and to control the activation energy of the cyclization. In good agreement with this notion and the fact that the developing radical centers are orthogonal to the out-of-plane π -system, the activation energies of thermal cycloaromatization reactions display low sensitivity to properties of the out-of-plane π -system, such as the presence of remote substituents.

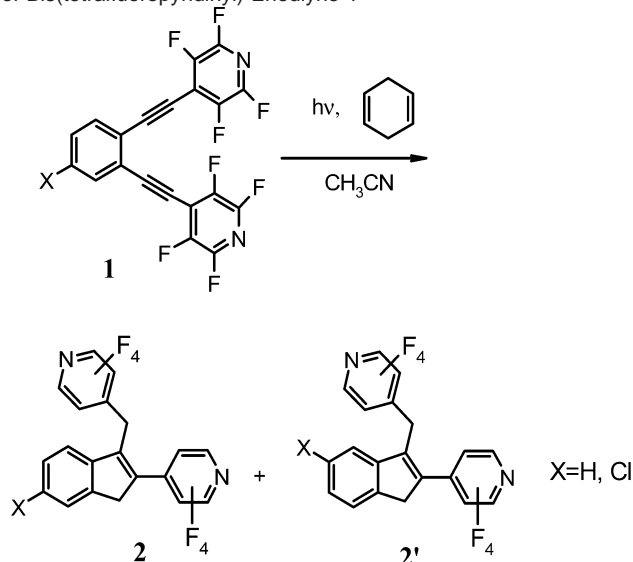
In this paper, we will show that the situation is changed and the role of the out-of-plane π -system becomes more important during radical-anionic cycloaromatization reactions. We also report our theoretical prediction of large substituent effects in radical anionic cycloaromatization reactions as well as the first detailed theoretical study of these processes. There are only a few experimental examples of such reactions,^{18,19} including our recent report of the photochemical C1–C5 cyclization of substituted enediyne—the process which ultimately leads to four formal H atom abstractions from organic substrates²⁰ and, thus, shows promise in the design of powerful DNA-damaging warheads (Scheme 1).²¹ Although many details of the reaction

mechanism are still under investigation, there is significant circumstantial evidence, e.g. incorporation of two deuterium atoms (one at each CH₂ groups of the indene **2**) in the presence of CH₃OD, which provides strong indication of a radical-anionic mechanism. Interestingly, the cyclization of unsymmetrically substituted enediyne is regioselective (e.g. when X = Cl, the ratio of **2** to **2'** is 9/1), indicating a considerably larger sensitivity to substituent effects than in the Bergman cyclization (Scheme 2).²²

These experimental results raise several questions. Why is the radical-anionic C1–C5 cyclization more feasible energetically? Is radical-anionic stabilization unique for the C1–C5 pathway? How does one-electron reduction influence the kinetics and thermodynamics of the Bergman (C1–C6) cyclization? What are the scope and limitations of radical-anionic cycloaromatization reactions? How may one control efficiency of these processes? How does the nature of substituents influence the cyclization? To address these questions, we studied two archetypical radical-anionic cyclizations of enediyne computationally. The results of this study are reported below.

(15) Haberhauer, G.; Gleiter, R. *J. Am. Chem. Soc.* **1999**, *121*, 4664–4668.
 (16) Galbraith, J. M.; Schreiner, P. R.; Harris, N.; Wei, W.; Wittkopp, A.; Shaik, S. *Chem. Eur. J.* **2000**, *6*, 1446.
 (17) Recently, we suggested that a more efficient way to control the Bergman cyclization involves interaction of the *in-plane* acetylenic orbitals with spatially proximal ortho substituents: Alabugin, I. V.; Manoharan, M.; Kovalenko, S. V. *Org. Lett.* **2002**, *4*, 1119.

(18) Whitlock and co-workers found that 1,2-bis(phenylethynyl)benzene undergoes cyclization with formation of a fulvene dianion when treated with lithium naphthalide in THF. It is conceivable that this reaction, in fact, proceeds through formation of a radical anion followed by facile cyclization and reduction of the same fulvene radical-anion intermediate as in our photochemical C1–C5 cyclization: Whitlock, H. W.; Sandvick, P. E.; Overman, L. E.; Reichard, P. B. *J. Org. Chem.* **1969**, *34*, 879.
 (19) For a radical-anionic cyclization of cross-conjugated enediyne see: Eshdat, L.; Berger, H.; Hopf, H.; Rabinovitz, M. *J. Am. Chem. Soc.* **2002**, *124*, 3822.
 (20) Alabugin, I. V.; Kovalenko, S. V. *J. Am. Chem. Soc.* **2002**, *124*, 9052.
 (21) (a) A topologically similar but mechanistically different C1–C5 cyclization of enediyne radical cations was also reported: Ramkumar, D.; Kalpana, M.; Varghese, B.; Sankararaman, S.; Jagadeesh, M. N.; Chandrasekhar, J. *J. Org. Chem.* **1996**, *61*, 2247. (b) Note, however, that subsequently this reaction was shown to proceed (at least in some cases) through an acid-catalyzed mechanism: Schmittel, M.; Kia, S. *Liebigs. Ann./Recl.* **1997**, 1391. (c) For more information on radical-cationic cycloaromatization reactions see also: Wandel, H.; Wiest, O. *J. Org. Chem.* **2002**, *67*, 388. (d) For a related triplet rearrangement of *ene yne allenene* see: Schmittel, M.; Rodríguez, D.; Steffen, J.-P. *Angew. Chem., Int. Ed.* **2000**, *39*, 2152. (e) For a triplet cyclization of diethynyl-diphenylmethanes see: Zimmerman, H. E.; Pincock, J. *J. Am. Chem. Soc.* **1973**, *95*, 3246. (f) Finally, an interesting computational analysis which discussed a possibility of *m*-benzyne rearrangement to five-membered products can be found in: Sander, W.; Exner, M.; Winkler, M.; Balster, A.; Hjerpe, A.; Kraka, E.; Cremer, D. *J. Am. Chem. Soc.* **2002**, *124*, 13072.
 (22) Although two regioisomers are indistinguishable for the Bergman cyclization, substituent effects can be estimated by comparison of the relative cyclization rates of unsubstituted vs substituted enediyne. See ref 17 for a discussion.

Scheme 2. Regioselectivity of Photochemical C1–C5 Cyclization of Bis(tetrafluoropyridinyl) Eneidyne 1

Computational Details and Choice of Method

Although multiconfigurational methods capable of accounting for electron correlation are generally needed for accurate description of such reactions,^{23–27} Density Functional (DFT) methods were successfully used to describe a number of cycloaromatization reactions.^{14b,17,25d–i,26,27} We have tested the applicability of two broken-spin unrestricted DFT methods (UB3LYP and UBLYP) which were recently used for computational studies of the Bergman and related cycloaromatization reactions by comparison with coupled-cluster computations using the Brueckner doubles ansatz (BD(T))²⁸—a method that provides a very accurate description of the thermal Bergman cyclization.²⁷ The computational results for the parent eneidyne at the DFT and BD(T) levels of theory are given in Table 1. For the radical-anionic cyclizations of the parent eneidyne, the BLYP/6-31+G* level of theory provides activation energies that are very close to those produced by the much more computationally expensive BD(T) computations. While the BLYP/6-31+G* level is the most accurate for describing the cyclizations per

Table 1. Activation Barriers and Reaction Energies (kcal mol⁻¹) of C1–C6 and C1–C5 Cyclizations of the Radical Anion of (Z)-Hex-3-ene-1,5-diyne Calculated at the UB3LYP (UBLYP) and BD(T) Levels^d

Basis set	$\Delta E^\ddagger(\text{A})$	$\Delta E_r(\text{A})$	$\Delta E^\ddagger(\text{B})$	$\Delta E_r(\text{B})$
Eneidyne (1)				
6-31G**	31.2 (25.4)	3.3 (6.8)	46.1 (41.6)	40.1 (41.1)
6-31+G*	31.0 (25.5)	4.6 (8.0)	46.5 (42.3)	41.2 (42.0)
6-311+G**	34.2 (28.5)	10.0 (13.4)	49.8 (46.3)	45.7 (45.1)
BD(T) ^a	29.2 (28.6)		41.4 (40.4)	
Eneidyne radical anion (1⁻)				
6-31G**	29.5 (26.9)	-16.7 (-16.1)	34.0 (31.1)	11.9 (11.7)
6-31+G*	27.0 (24.5)	-19.4 (-18.4)	31.3 (28.5)	9.6 (9.6)
6-311+G**	28.7 (25.9)	-14.8 (-14.1)	33.3 (30.4)	13.5 (13.4)
BD(T) ^a	24.4 (24.2)		28.9 (28.2)	
Solvent ^b	25.4 (22.9)	-24.9 (-26.5)	29.4 (26.8)	7.2 (7.0)
Solvent ^c	23.4 (21.0)	-26.4 (-27.6)	31.5 (28.7)	9.6 (9.4)
Triplet Eneidyne (3¹)				
6-31G**	23.7 (19.5)	-45.2 (-39.7)	38.0 (32.1)	-5.2 (-0.9)
6-31+G*	23.8 (19.8)	-43.7 (-37.9)	37.2 (31.3)	-4.0 (-1.2)
6-311+G**	25.7 (21.7)	-39.1 (-33.3)	39.8 (34.4)	-0.2 (-2.8)
BD(T) ^a	19.4 (19.0)		34.5 (36.3)	

^a Single-point computations with the 6-31G** basis set on the B3LYP(BLYP)/6-31G** geometry. ^b Optimization at the DFT(SCRF-PCM)/6-31G** level with acetonitrile solvent. ^c Optimization at the DFT(SCRF-PCM)/6-31+G* level with acetonitrile solvent. ^d The best theoretical methods are highlighted in boldface.

se, the *relative* trends in the activation energies are equally well reproduced by B3LYP/6-31G** computations (see the Supporting Information). Because the more general B3LYP level is likely to be more accurate in describing substituent effects and in order to allow comparison with the respective thermal cyclizations,¹⁷ we have selected the B3LYP/6-31G** level as a basic level for this paper. In most cases, we also ran a parallel set of computations at the BLYP/6-31G** level. Because diffuse functions are generally needed when higher accuracy in the description of anionic species is desired, we limited the use of the 6-31G** basis set only for the cases dealing with relative or qualitative trends in reactivity. More information on the basis sets effects can be found in the Supporting Information.

All stationary points were completely characterized using frequency analysis. The internal reaction coordinate (IRC) computations were performed using the IRC option in Gaussian 98. The electronic structures of the IRC points were analyzed using natural bond orbital (NBO) analysis.²⁹ The NBO analysis involves sequential transformation of nonorthogonal atomic orbitals (AOs) to the complete and orthonormal sets of “natural” atomic orbitals (NAOs), hybrid orbitals (NHOs), and bond orbitals (NBOs). These localized basis sets describe the electron density and other properties by the smallest number of filled orbitals in the most rapidly convergent fashion. These orbitals are closely related to the localized orbitals (bonds and lone pairs) used by organic chemists and, thus, become increasingly useful in translating quantum-mechanical results into the language of organic chemistry.³⁰

Results and Discussion

Radical-Anionic Cyclizations of Parent Eneidyne 3. A. Energies. The thermal Bergman cyclization of parent eneidyne

- (23) (a) Scheiner, A. C.; Schaefer, H. F., III; Liu, B. *J. Am. Chem. Soc.* **1989**, *111*, 3118. (b) Nicolaidis, A.; Borden, W. T. *J. Am. Chem. Soc.* **1993**, *115*, 11951. (c) Lindh, R.; Persson, B. J. *J. Am. Chem. Soc.* **1994**, *116*, 4963. (d) Lindh, R.; Lee, T. J.; Bernhardsson, A.; Persson, B. J.; Karlström, G. *J. Am. Chem. Soc.* **1995**, *117*, 7186. (e) Kraka, E.; Cremer, D.; Bucher, G.; Wandel, H.; Sander, W. *Chem. Phys. Lett.* **1997**, *268*, 313. (f) Lindh, R.; Ryde, U.; Schütz, M. *Theor. Chem. Acta* **1997**, *97*, 203. (g) McMahon, R. J.; Halter, R. J.; Fimmen, R. L.; Wilson, R. J.; Peebles, S. A.; Kuczkowski, R. L.; Stanton, J. F. *J. Am. Chem. Soc.* **2000**, *122*, 939. (h) Jones, G. B.; Warner, P. M. *J. Am. Chem. Soc.* **2001**, *123*, 2134.
- (24) Cramer, C. J.; Nash, J. J.; Squires, R. R. *Chem. Phys. Lett.* **1997**, *277*, 311. Cramer, C. J.; Nash, J. J.; Squires, R. R. *Chem. Phys. Lett.* **1997**, *277*, 311. Cramer, C. J.; Squires, R. R. *J. Phys. Chem. A* **1997**, *101*, 9191. Wierschke, S. G.; Nash, J. J.; Squires, R. R. *J. Am. Chem. Soc.* **1993**, *115*, 11958. Cramer, C. J. *J. Am. Chem. Soc.* **1998**, *120*, 6261. Johnson, W. T. G.; Sullivan, M. B.; Cramer, C. J. *Int. J. Quantum Chem.* **2001**, *85*, 492–508. Johnson, W. T. G.; Cramer, C. J. *J. Phys. Org. Chem.* **2001**, *14*, 597–603. Cramer, C. J.; Thompson, J. J. *J. Phys. Chem. A* **2001**, *105*, 2091–2098. Feldgus, S.; Shields, G. C.; *Chem. Phys. Lett.* **2001**, *347*, 505–511.
- (25) (a) Logan, C. F.; Chen, P. *J. Am. Chem. Soc.* **1996**, *118*, 2113. (b) Schottelius, M. J.; Chen, P. *J. Am. Chem. Soc.* **1996**, *118*, 4896. (c) Hoffner, J.; Schottelius, J.; Feichtinger, D.; Chen, P. *J. Am. Chem. Soc.* **1998**, *120*, 376–385. (d) Kraka, E.; Cremer, D. *J. Am. Chem. Soc.* **2000**, *122*, 8245. (e) Kraka, E.; Cremer, D. *J. Comput. Chem.* **2001**, *22*, 216–229. (f) Grafenstein, J.; Hjerpe, A. M.; Kraka, E.; Cremer, D. *J. Phys. Chem. A* **2000**, *104*, 1748. (g) Ahlstrom, B.; Kraka, E.; Cremer, D. *Chem. Phys. Lett.* **2002**, *361*, 129. (h) Stahl, F.; Moran, D.; Schleyer, P. v. R.; Prall, M.; Schreiner, P. R. *J. Org. Chem.* **2002**, *67*, 1453. (i) De Profit, F.; Schleyer, P. v. R.; Lenthe, J. v. H.; Stahl, F.; Geerlings, P. *Chem. Eur. J.* **2002**, *8*, 3405.
- (26) Schreiner, P. R. *J. Am. Chem. Soc.* **1998**, *120*, 4184. Schreiner, P. R. *Chem. Commun.* **1998**, 483.
- (27) Prall, M.; Wittkopp, A.; Schreiner, P. R. *J. Phys. Chem. A* **2001**, *105*, 9265.
- (28) Brueckner, K. A. *Phys. Rev.* **1954**, *96*, 508–516. Stanton, J. F.; Gauss, J.; Bartlett, R. J. *J. Chem. Phys.* **1992**, *97*, 5554.

- (29) The NBO 4.0 program: Glendening, E. D.; Badenhoop, J. K.; Reed, A. E.; Carpenter, J. E.; Weinhold, F. F. Theoretical Chemistry Institute, University of Wisconsin, Madison, WI, 1996.

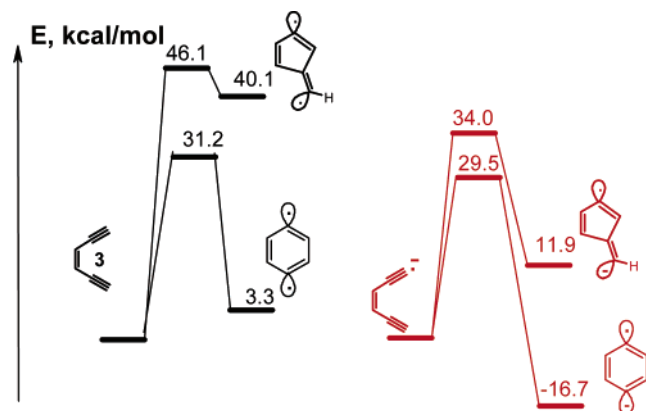


Figure 1. Reaction energy profiles for thermal (on the left) and radical-anionic (on the right) C1–C6 and C1–C5 cyclizations of the parent enediyne **3** computed at the B3LYP/6-31G** level.

3 proceeds only at significantly elevated temperatures,² whereas thermal C1–C5 cyclization is a process which should be virtually impossible to observe (*vide infra*).²⁷ The situation changes dramatically upon one-electron reduction of the enediyne moiety. At all levels of theory, calculated activation energies for both C1–C5 and C1–C6 cyclization pathways of parent enediyne **3** are significantly lower than those of their thermal counterparts (Table 1). The effect is much more pronounced for the C1–C5 pathway (>12 kcal/mol at the most accurate BD(T)/6-31G** level), but the activation energy of the C1–C6 (the Bergman) cyclization is also decreased quite significantly (>4 kcal/mol at the BD(T)/6-31G** level), to the extent where it may proceed (albeit slowly) even at room temperature.

Changes in the reaction thermodynamics for both processes are even larger (Figure 1). The endothermicity of the C1–C5 cyclization decreases by ca. 30 kcal/mol and, thus, becomes

comparable with that of the thermal Bergman cyclization. This observation is in drastical contrast with the *thermal* C1–C5 cyclization first studied computationally by Schreiner,²⁷ who found the potential minimum for the singlet fulvene diradical to be so shallow that this diradical is expected to reopen to the starting enediyne rather than abstract a hydrogen atom.

The radical-anionic C1–C6 (Bergman) cyclization shows a similar response to one-electron reduction, which renders this reaction highly *exothermic*. On the basis of these results, the radical-anionic Bergman cyclization is expected to be a highly efficient and essentially irreversible reaction, in contrast to the thermal Bergman cyclization, which is endothermic and readily reversible.

B. Geometry Changes upon One-Electron Reduction of Eneidyne and Further along the Cycloaromatization Processes.

The significant geometric changes of the enediyne moiety upon one-electron reduction reflect large changes in the electronic structure (Figure 2). Most noticeably, both C3–C4 (formerly the double bond) and C1–C2 (formerly the triple bond) distances become larger, indicating a decrease in π -bonding between the corresponding atoms. In contrast, the C2–C3 distance shortens to the value typical for a double bond. Both C1–C5 and C1–C6 distances increase due to outward bending of the C1–C2 bond—a direct result of increased electron repulsion. In addition, the enediyne radical anions are not completely planar—hydrogen atoms at terminal carbons deviate from the plane formed by the enediyne moiety.

All these changes agree well with the reductive population of the enediyne LUMO, which has a nodal structure corresponding to the bis(allyl) moiety with two nonbonding centers at the terminal carbon atoms given in Figure 3. As expected, increase in π -bond order upon one-electron reduction leads to

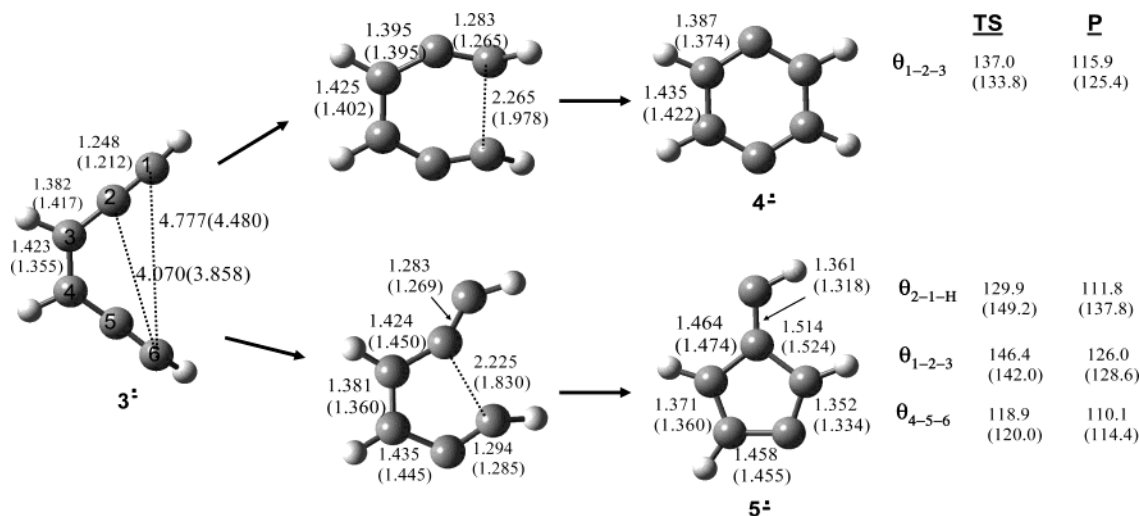


Figure 2. B3LYP/6-31G** geometries of reactants, transition states, and products of the radical-anionic C1–C6 and C1–C5 cyclizations of (*Z*)-hex-3-ene-1,5-diyne. Bond lengths are given in Å, and valence angles are given in deg. For comparison, the values for the diradical pathway are given in parentheses.

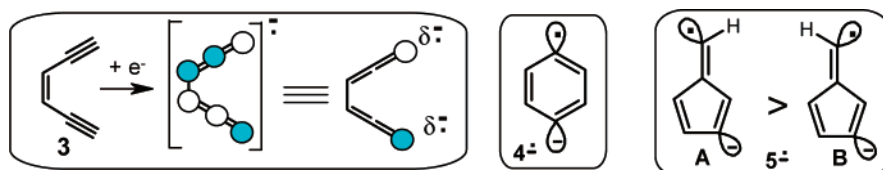
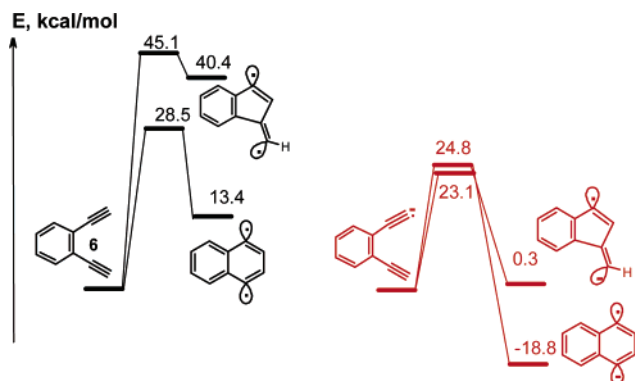
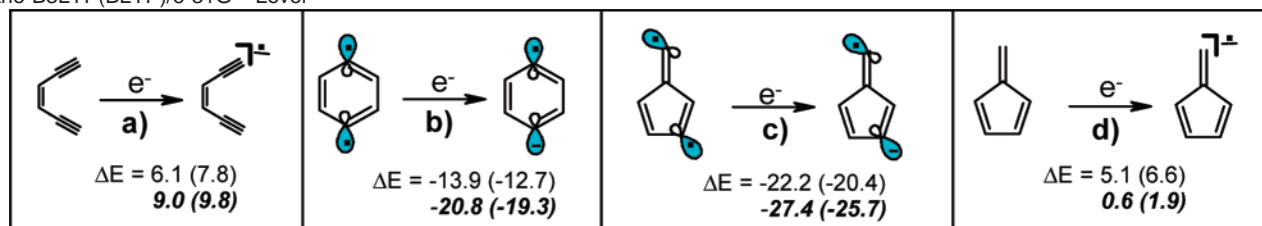


Figure 3. Dominant Lewis structure of the enediyne radical anion, *p*-benzyne radical anion and 1,5-dehydrofulvene radical anion. The dehydrofulvene “trans” isomer **A** is 2.7 kcal/mol more stable than the “cis” isomer **B** (see also ref 27).

Scheme 3. Electron Affinities of Parent and Benzannellated Eneidyynes (in Bold Italics) and Corresponding Fulvene Diradicals and Fulvenes at the B3LYP(BLYP)/6-31G** Level**Figure 4.** Reaction energy profiles for thermal (on the left) and radical-anionic (on the right) C1–C6 and C1–C5 cyclizations of the benzannellated eneidyne **6** computed at the B3LYP/6-31G** level.³²

a decrease in the corresponding C–C distances in the radical anion, whereas a decrease in the π -bond order has the opposite effect. The decrease in conjugation of π -orbitals at the terminal carbons with the rest of the *out-of-plane* π -system along with the concomitant increase in the net electron density on these atoms lead to “pyramidalization” of terminal carbon atoms. The “pyramidalization” is likely to play an important role in accessing crossing between electronic configurations with either an *out-of-plane* or an *in-plane* singly occupied MO (SOMO) which occurs along the reaction path (vide infra).

As both C1–C5 and C1–C6 cyclizations proceed, the geometric differences between stationary points at radical-anionic and diradical pathways diminish. The largest differences are the considerably larger incipient C1–C6 (C1–C5) distances for radical-anionic cyclizations. This indicates much earlier transition states and is in accord with the Hammond postulate. Almost all carbon–carbon distances in products are larger for the radical anions, but the differences are not dramatic except for the endocyclic double bond in fulvene **5**, which is noticeably lengthened in the corresponding radical anion.

2. Radical-Anionic Cyclizations of Benzannellated Eneidyynes. A. Energies. Cycloaromatization reactions of benzannellated eneidyynes are also accelerated by one-electron reduction, but the effects are much larger than for the simple eneidyne **3**.³¹ In fact, for *benzannellated* eneidyynes the activation energy for both anionic cyclizations is close to the threshold for spontaneous cyclization at ambient conditions (Table 3 and Figure 4). The largest practical difference between the two pathways is that the thermoneutral C1–C5 cyclization should be readily reversible at ambient temperatures, whereas the highly exothermic C1–C6 pathways should be essentially irreversible under the same conditions. Interestingly, both reductive cyclizations are predicted to be highly sensitive not only to benzannellation per se but also to π -conjugative effects of remote

substituents in the aromatic rings (these substituent effects will be discussed in detail in section 4).

B. Geometries. Although the general structural changes accompanying the cyclizations of benzannellated eneidyynes parallel the changes in the analogous cyclization of parent eneidyne **3**, there are some interesting differences. The largest of these is that considerably earlier transition states for more exothermic C1–C5 and C1–C6 cyclizations of 1,2-dithiynylbenzene **6** are characterized by longer incipient C1–C5 and C1–C6 bond lengths.

Most of the other bonds in benzannellated species are also slightly lengthened compared with those in their prototypes derived from **3**. The largest elongation is observed for the central (C3–C4) bond of the eneidyne moiety. Interestingly, even despite the longer C3–C4 distance, the C1–C6 (and C1–C5) distances in the benzannellated eneidyne radical anion are shorter than in the radical anion derived from the parent eneidyne **3**. On the other hand, C1–C6 and, especially, C3–C4 bonds in the dehydronaphthalene product of radical-anionic C1–C6 cyclization are remarkably long. Another interesting feature is further elongation of the C1–C5 bond in the benzannellated fulvene radical anion compared with the already quite long C1–C5 bond in fulvene radical anion **5**. On the other hand, the exocyclic double bond is shorter in the benzfulvene product than in fulvene **5**. Radical anions derived from benzannellated eneidyynes are also noticeably nonplanar.

3. Electronic Effects in Radical-Anionic Cyclizations. A. Global Changes: Reactant Destabilization vs Product Stabilization. In principle, the increased exothermicity of the radical-anionic cyclizations can stem from two alternative sources: reactant destabilization or product stabilization. The relative importance of these effects can be expediently estimated using the calculated electron affinities given in Scheme 3.

(30) For an illustrative rather than an exhaustive list of recent applications of the NBO method for analysis of chemical bonding, see: Reed, A. E.; Weinhold, F. *Isr. J. Chem.* **1991**, *31*, 277. Weinhold, F. *Theochem-J. Mol. Struct.* **1997**, 398, 181. Goodman, L.; Pophristic, V.; Weinhold, F. *Acc. Chem. Res.* **1999**, *32*, 983. Goodman, L.; Pophristic, V. *T. Nature* **2001**, *411*, 565. Salzner, U.; Schleyer P. v. R. *J. Org. Chem.* **1994**, *59*, 2138. Gleiter, R.; Lange, H.; Borzyk, O. *J. Am. Chem. Soc.* **1996**, *118*, 4889. Freeman, F.; Lee, K.; Hehre W. J. *Struct. Chem.* **2002**, *13*, 149. Klod, S.; Koch, A.; Kleinpeter, E. *J. Chem. Soc., Perkin Trans. 2* **2002**, 1506. Alabugin, I. V.; Zeidan, T. A. *J. Am. Chem. Soc.* **2002**, *124*, 3175. Wilkens, S. J.; Westler, W. M.; Weinhold, F.; Markley, J. L. *J. Am. Chem. Soc.* **2002**, *124*, 1190. van der Venken, B. J.; Herrebout, W. A.; Szostak, R.; Shchepkin, D. N.; Havlas, Z.; Hobza, P. *J. Am. Chem. Soc.* **2001**, *123*, 12290. Lewis, B. E.; Schramm, V. L. *J. Am. Chem. Soc.* **2001**, *123*, 1327. Cortes, F.; Tenorio, J.; Collera, O.; Cuevas, G. *J. Org. Chem.* **2001**, *66*, 2918. Sadlej-Sosnowska, N. *J. Org. Chem.* **2001**, *66*, 8737. Uddin, J.; Boehme, C.; Frenking, G. *Organometallics* **2000**, *19*, 571. Gilbert, T. M.; *Organometallics* **2000**, *19*, 1160. Munoz, J.; Sponer, J.; Hobza, P.; Orozco, M.; Luque, F. J. *J. Phys. Chem. B* **2001**, *105*, 6051. Alabugin, I. V. *J. Org. Chem.* **2000**, *65*, 3910. Xie, Y.; Grev, R. S.; Gu, J.; Schaefer, H. F., III; Schleyer, P. v. R.; Su, J.; Li, X.-W.; Robinson, G. H. *J. Am. Chem. Soc.* **1998**, *120*, 3773. Paddon-Row: M. N.; Shephard, M. J. *J. Am. Chem. Soc.* **1997**, *119*, 5355.

(31) Note that benzannellation does not have a large effect on activation energy for the cyclization step of thermal (diradical) cycloaromatization reactions.

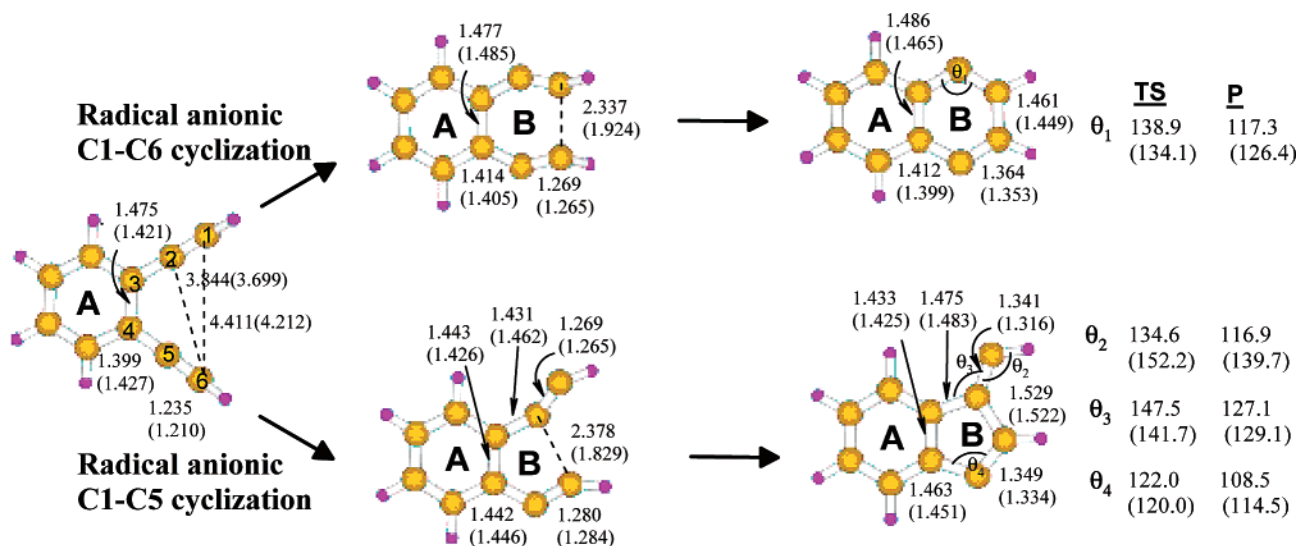


Figure 5. B3LYP/6-31G** geometries of reactants, transition states, and products of the radical anionic C1–C6 and C1–C5 cyclizations of benzannelated enediyne **6** (bond lengths are in Å, and angles are in deg). Values in parentheses correspond to the respective diradical cyclizations.

The reduction of enediyne (**a** in Scheme 3) is only ca. 1 kcal/mol more endothermic than that of fulvene (**d**), but benzannelation significantly increases the difference in reduction potentials between fulvenes and enediynes. Reduction of both *p*-benzyne and dehydrofulvene diradicals (**b** and **c**) is strongly exothermic, especially for the benzannelated cases. These results clearly suggest that increased stability of the products is the largest component of higher reaction exothermicity but the role of reactant destabilization is also significant. Interestingly, both factors also contribute to an additional increase in exothermicity for the cyclizations of benzannelated enediyne **6** (5.2 kcal/mol of extra product stabilization vs 2.9 kcal/mol of reactant destabilization). The electron affinity of the benzannelated fulvene is larger than that of fulvene itself (difference of 4.5 kcal/mol) and much larger than for the reactant enediynes, which explains why the fulvene intermediates readily undergo further photoreduction under the reaction conditions in Scheme 1.

The global energy effects above can be dissected into contributions from several effects: (a) aromaticity in the newly formed rings B (Figure 5), (b) dynamic interplay of aromaticity/antiaromaticity in rings A (Figure 5) present in the reactants and conserved in the products, and (c) increased coupling between nonbonding orbitals. To understand the relative importance of the above effects, we need to discuss the crossing of *in-plane* and *out-of-plane* molecular orbitals (MOs) of the reactant in the vicinity of the TS. This MO crossing is crucial for an understanding of radical-anionic cycloaromatization reactions.

B. Molecular Orbital Analysis. Figure 6 illustrates an extremely important and general feature of cycloaromatization reactions which, to the best of our knowledge, has not been considered before, namely, two crossings (one for occupied, one for virtual MOs) between the out-of-plane and in-plane MOs. These MO crossings directly result from bond-forming interaction of the two *in-plane* π -orbitals that transforms them into a σ -bond and a pair of nonbonding MOs (two radical centers for the thermal cyclizations).³³ Consequently, in the vicinity of the TS one of the unoccupied *in-plane* MOs (reactant LUMO+1 for the C1–C6 cyclization or reactant LUMO+2 for the C1–C5 cyclization) is stabilized to the extent that it becomes the

new LUMO. In other words, in the reactant both HOMO and LUMO correspond to *out-of-plane* orbitals but at the shorter C1–C6 or C1–C5 distances the frontier MOs are localized in *in-plane* nonbonding (radical) orbitals. These crossings are not important for the thermal cycloaromatization reactions but become essential for reactions which either depopulate the HOMO or/and populate the LUMO of the enediyne moiety (oxidation, reduction, or photochemical excitation), as described below.

Although one-electron reduction of the enediyne moiety populates the (out-of-plane) LUMO of the enediyne, the electron “hops” to the new (in-plane) LUMO after this MO crossing, and as a result, the excess of negative charge is transferred to orbitals orthogonal to the *out-of-plane* π -system. Such a switch in MO populations should proceed through a crossing between electronic configurations with either an *out-of-plane* or an *in-plane* singly occupied MO (SOMO) along the reaction path. The position and relative energy of this crossing are directly related to those for the activation barrier for the reaction. This notion provides a key to efficient control of radical-anionic cycloaromatization reactions (see the following section for a more detailed discussion).

The close relationship between the reaction TS and the above MO crossing is also in an excellent agreement with Natural Bond Orbital (NBO) analysis which provides “the best Lewis structure” of intermediate structures along the internal reaction (IRC) pathway for the cyclizations. Results of the NBO analysis in Figure 7 illustrate that the dominant Lewis structure corresponds to the extra electron being in an out-of-plane MO for the IRC points before the TS and that the change in the dominant

(32) The starting points for both C1–C5 and C1–C6 cyclizations are characterized using C1–C6 distances to stress that the starting point for both cyclizations is the same enediyne radical anion. However, for transition states and products of C1–C5 and C1–C6 cyclizations, the respective incipient bond length (C1–C5 or C1–C6) was used as the reaction coordinate.

(33) Such crossings are common for reactions where chemical bonds are either transformed into free radicals, e.g. for photochemical Norrish type I reactions, or simply stretched and weakened, e.g. electrocyclic ring opening (see for example: Rondan, N. G.; Houk, K. N. *J. Am. Chem. Soc.* **1985**, *107*, 2099. Dolbier, W. R.; Koroniak, H.; Houk, K. N.; Sheu, C. *Acc. Chem. Res.* **1996**, *29*, 471).

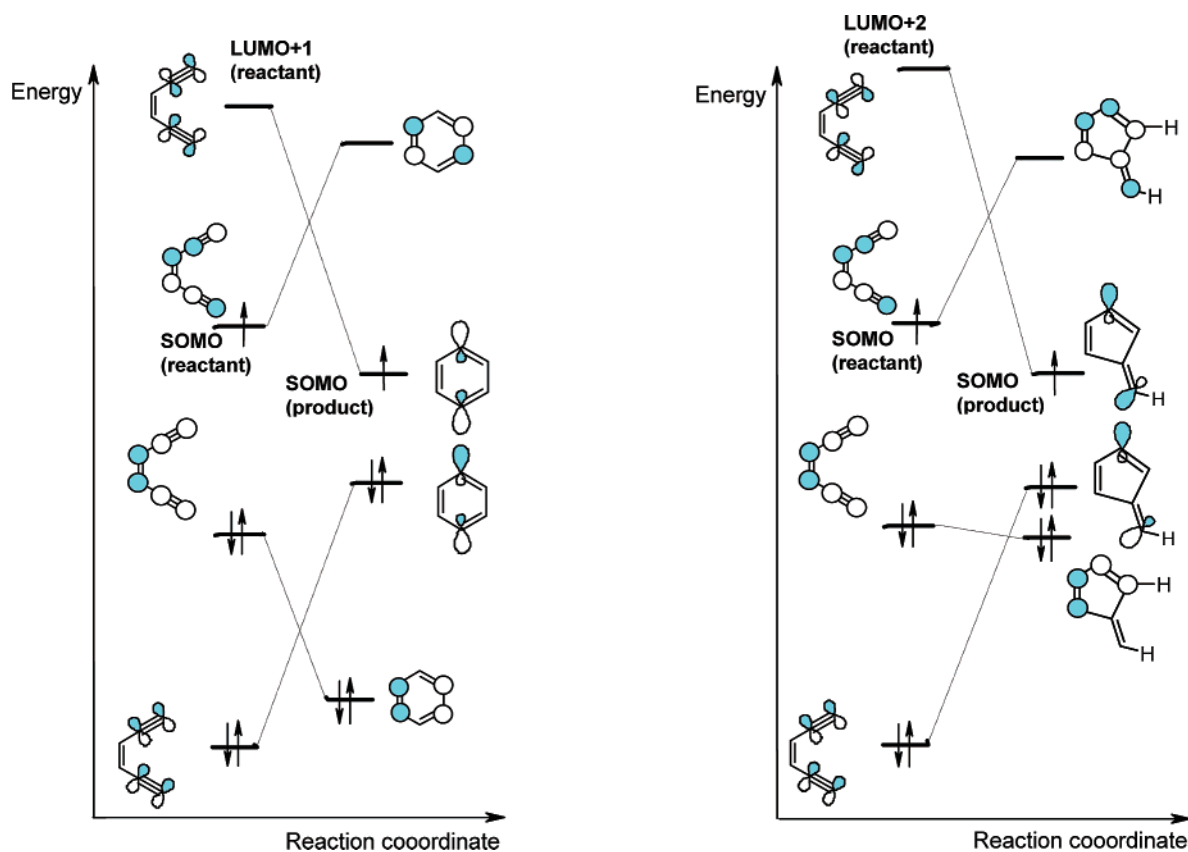


Figure 6. Crossings of *in-plane* and *out-of-plane* frontier MOs in the radical-anionic Bergman and C1–C5 cyclizations.

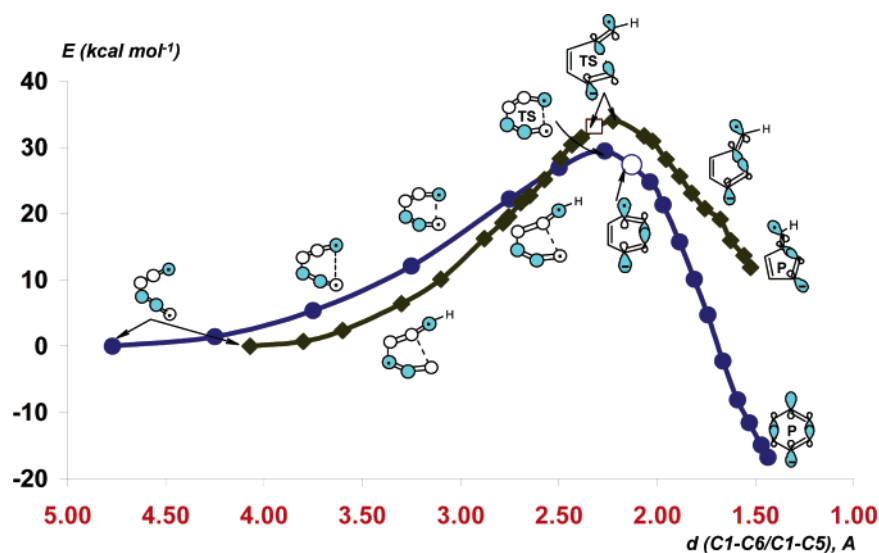


Figure 7. Dominant NBO structures along the IRC pathways of the C1–C5 (diamonds) and C1–C6 (circles) radical anionic cyclizations that show the “hopping of electron” from an *out-of-plane* to an *in-plane* MO in the vicinity of TS (B3LYP/6-31G** level). IRC points where the dominant Lewis structure changes are shown as a white square (C1–C5 cyclizations) and white circle (C1–C6 cyclization).

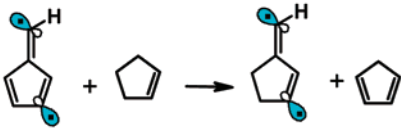
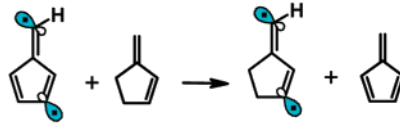
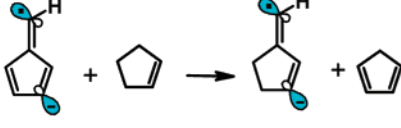
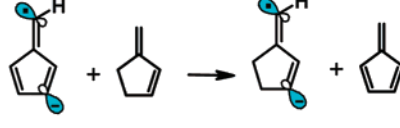
NBO Lewis structure (“the electron hop”) coincides almost exactly with the TS.

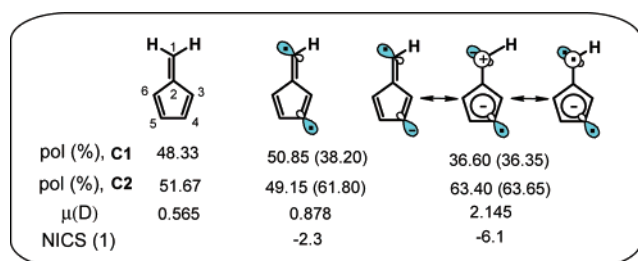
C. Aromaticity. There are two parameters related to the changes in aromaticity during the C1–C6 and C1–C5 cyclizations. First, a new aromatic ring is formed in both cyclizations. The energetic benefits due to aromaticity in the new ring are much larger for the C1–C6 cyclization³⁴ (where a benzene ring is formed) than in the C1–C5 cyclization, where the new ring

is better described as a highly polarized fulvene moiety rather than a pentadienyl anion. The extra electron populates an *in-plane* nonbonding MO rather than a π^* -orbital of the fulvene moiety, as illustrated in Figure 3; thus, the negative charge is mainly distributed among the *in-plane* MOs. However, the relative NBO polarizations of the exocyclic C1–C2 bond in fulvene, dehydrofulvene diradical, and dehydrofulvene radical anion given in Figure 8 show increased bond polarization in the radical anion which is consistent with the larger contribution of an aromatic resonance structure.

(34) Aromaticity effects in *thermal* cycloaromatization reactions were thoroughly studied by Stahl et al. and De Proft et al. in refs 25i,h.

Table 2. Aromatic Stabilization Energies (kcal mol⁻¹) for the Products of Thermal and Radical-Anionic C1–C5 Cyclizations Calculated at Various DFT Levels

Equation	Method	ΔE	Equation	ΔE
	B3LYP/6-31G**	-2.5		-1.5
	BLYP/6-31G**	-2.2		-1.3
	BLYP/6-31+G*	-3.0		-1.9
	B3LYP/6-31G**	5.4		6.1
	BLYP/6-31G**	5.5		6.4
	BLYP/6-31+G*	4.6		5.7

**Figure 8.** NBO polarization of the exocyclic C1–C2 double bond in fulvene, dehydrofulvene diradical, and dehydrofulvene radical anion, dipole moments of these species (B3LYP/6-31G** level), and NICS(1) values computed at the B3LYP/6-311+G**/B3LYP/6-31G** level 1 Å above the ring center. Spin polarization in the radical species results in different polarizations of the exocyclic double bond for α - and β -spin electron systems. Values for the β spin are shown in parentheses.

Aromaticity in the new five-membered ring is substantial, as evident from isodesmic reactions, which compare relative stabilizations of fulvene diradical and radical anions using cyclopentadiene and fulvene as reference points (Table 2). While the diradical is slightly destabilized compared with the parent hydrocarbons, the radical anion displays increased stability. The additional stabilization of fulvene radical anion **5** relative to the fulvene diradical is ca. 7–8 kcal/mol and, thus, is a noticeable contribution to the larger exothermicity of the radical anionic pathway.

The second parameter important for the cyclizations of benzannelated enediyne is aromaticity in the benzene ring **A** annealed to the enediyne moiety of the reactant. Adding an extra electron to the *out-of-plane* π -array diminishes aromaticity in this ring in the reactant enediyne radical anion, because the extra electron populates an out-of-plane MO with the nodal structure illustrated in Figure 9. As a result, the “best Lewis structure” of the enediyne radical anion provided by natural bond orbital (NBO)³⁵ analysis can be best described by the bis-allenic *o*-quinodimethide in Figure 9. Note that the NBO description is in excellent agreement with the nodal structure of the enediyne LUMO. At the MO crossing in the vicinity of the TS, the extra electron is transferred to the *in-plane* orbital, and aromaticity in the benzene ring is restored. Regaining aromaticity in the diradical products provides an additional driving force for these cyclizations. Thus, both C1–C6 and C1–C5 cyclizations of

benzannelated enediyne can be appropriately named cyclo-rearomatization reactions. Rearomatization in the vicinity of the TS makes radical-anionic reactions drastically different from their diradical counterparts and leads to dramatic increase in their efficiency. Although this is an unusual feature for a cycloaromatization reaction, restoration of aromaticity is well-recognized as a driving force for many other organic reactions, e.g. the second step of aromatic substitution reactions, Diels–Alder reactions of *o*-diquinones,³⁶ 1,5-hydrogen sigmatropic shifts in dehydrophenanthrene systems,³⁷ and many other examples.

This interpretation is supported by the results of nucleus-independent chemical shift (NICS)³⁸ analysis (Figure 10). The NICS value at a distance of 1 Å from the ring centers (NICS(1) value) is considered to be a reliable magnetic criterion of aromaticity/antiaromaticity.³⁸ Positive NICS values for the enediyne radical anion which indicate *antiaromaticity* of the reactant are changed to negative NICS values in the TS and the products of both C1–C5 and C1–C6 cyclizations. NICS(1) values in Figure 10 are in good agreement with energetic estimates of antiaromaticity from the isodesmic reaction in Scheme 4.

Another way to estimate the energetic consequences of decrease in aromaticity is by means of the isodesmic reaction in Scheme 4. Superficially, one would expect that a more extended π -system of the benzannelated enediyne would be able to accommodate an extra electron better than the parent enediyne, but the situation is just the opposite—the isodesmic reaction in Scheme 4 is endothermic.³⁹ Although the additional destabiliza-

- (35) Foster, J. P.; Weinhold, F. F. *J. Am. Chem. Soc.* **1980**, *102*, 7211. Reed, A. E.; Weinhold, F. F. *J. Chem. Phys.* **1983**, *78*, 4066. Reed, A. E.; Weinstock, F.; Weinhold, F. F. *J. Chem. Phys.* **1985**, *83*, 735. Reed, A. E.; Curtiss, L. A.; Weinhold, F. F. *Chem. Rev.* **1988**, *88*, 899. Weinhold, F. In *Encyclopedia of Computational Chemistry*; Schleyer P. v. R., Ed.; Wiley: New York, 1998; Vol. 3, p 1792.
- (36) Segura, J. L.; Martin, N. *Chem. Rev.* **1999**, *99*, 3199. Manoharan, M.; De Proft, F.; Geerlings, P. *J. Org. Chem.* **2000**, *65*, 7971.
- (37) Lewis, F. D.; Zuo, X.; Gevorgyan, V.; Rubin, M. *J. Am. Chem. Soc.* **2002**, *124*, 13664.
- (38) Schleyer, P. v. R.; Manoharan, M.; Wang, Z.-X.; Kiran, B.; Jiao, H.; Puchta, R.; van Eikema Hommes, N. J. R. *Org. Lett.* **2001**, *3*, 2465. Schleyer, P. v. R.; Jiao, H.; Hommes, N. J. R. v. E.; Malkin, V. G.; Malkina, O. L. *J. Am. Chem. Soc.* **1997**, *119*, 12669. Schleyer, P. v. R.; Maerker, C.; Dransfeld, A.; Jiao, H.; Hommes, N. J. R. v. E. *J. Am. Chem. Soc.* **1996**, *118*, 6317. For the seminal paper on using NICS for open-shell species, see: Gogonea, V.; Schleyer, P. v. R.; Schreiner, P. R. *Angew. Chem., Int. Ed.* **1998**, *37*, 1945–1948.

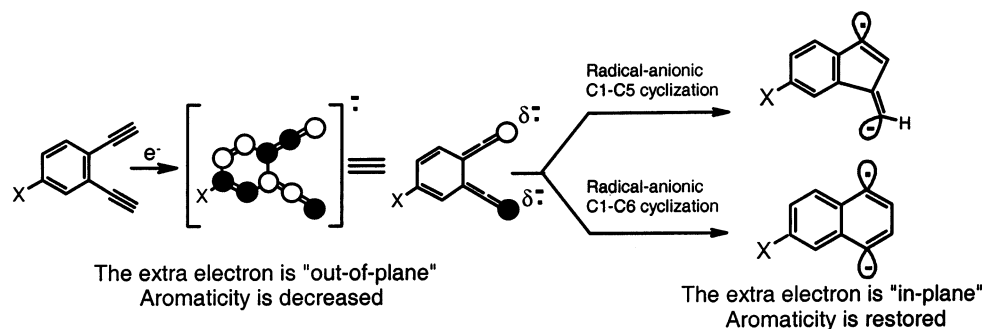


Figure 9. Changes in aromaticity of the benzene ring annealed to the central (C3–C4) bond of the enediyne moiety during the radical-anionic C1–C5 cyclization.

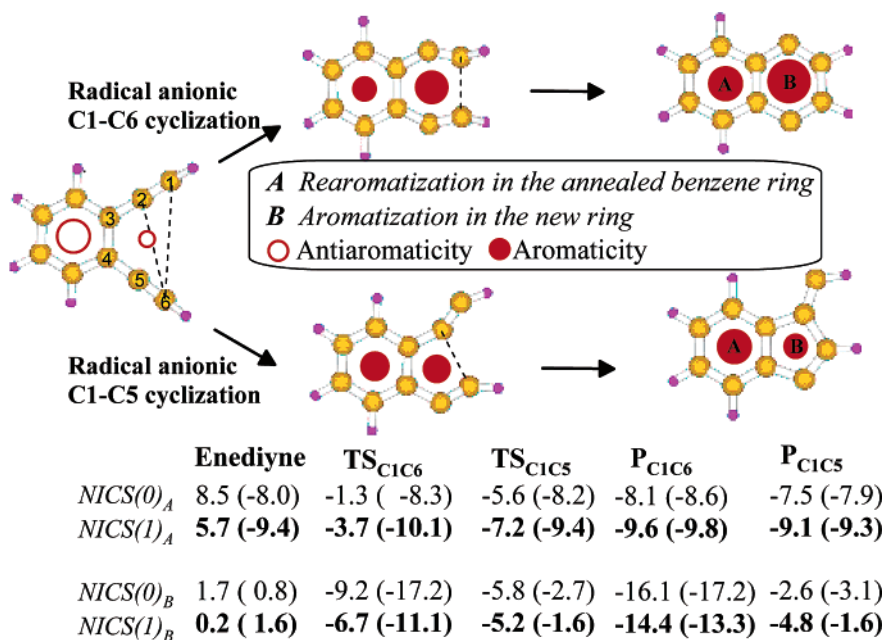
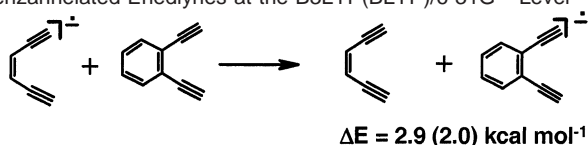


Figure 10. B3LYP/6-31G** NICS values (in ppm) in the plane of the ring (NICS(0)) and 1 Å above the ring (NICS(1)) for reactants, TSs, and products from the radical anionic C1–C6 and C1–C5 cyclizations of benzannelated enediyne **6**. The size of the red circle is proportional to the NICS(1) magnitude.

Scheme 4. Relative Stabilities of Radical Anions of Parent and Benzannelated Eneidyne at the B3LYP(BLYP)/6-31G** Level



tion is not large, one has to bear in mind that the radical anion of the parent enediyne itself is significantly destabilized by one-electron reduction and, thus, this reference point is relatively high in energy.

D. Electronic Coupling of Nonbonding Electrons (Through-Bond (TB) and Through-Space (TS)). Increased coupling between nonbonding orbitals in 1,4-radical anions is the other source of increased exothermicity of radical-anionic cycloaromatizations. There are two paths for coupling of the nonbonding electrons: direct coupling through space (TS) or indirect coupling through antibonding (σ^*) bridge orbitals (through-bond (TB) coupling).⁴⁰ The orbital interaction of the two σ radicals

through σ^* bridge orbitals plays an important role in the chemistry of 1,4-diradicals, as analyzed in a classic work by Hoffmann^{40a} (and more recently in much detail by others).^{25,41} The TB coupling is the most important for the diradical product of thermal Bergman cyclization, where it lowers the energy of the asymmetric combination of the nonbonding MOs below that of the corresponding symmetric combinations, which, in turn, renders this reaction symmetry allowed. UDFT biradical stabilization energies (BSEs) in *p*-benzynes are underestimated but are in qualitatively reasonable (especially at the BLYP level) agreement with an experimental estimate of ca. 5 kcal/mol and with a singlet/triplet gap of 3.8 kcal/mol.⁴² Not surprisingly,

(39) The endothermicity is relatively small which is due to the fact that electron reduction of the parent enediyne is also rather endothermic (a π^* orbital is populated and three formal *out-of-plane* double bonds in the NBO Lewis structure of the neutral enediyne are changed into a combination of two π -bonds and two nonbonding orbitals).

(40) (a) Hoffmann, R.; Imamura, A.; Hehre, W. J. *J. Am. Chem. Soc.* **1968**, *90*, 1499. (b) Hoffmann, R. *Acc. Chem. Res.* **1971**, *4*, 1–9. (c) Paddon-Row, M. N. *Acc. Chem. Res.* **1982**, *15*, 245. (d) Gleiter, R.; Schafer, W. *Acc. Chem. Res.* **1990**, *23*, 369–375. (e) Brodskaya, E. I.; Rátovskii, G. V.; Voronkov, M. G. *Russ. Chem. Rev. (Engl. Transl.)* **1993**, *62*, 975.
(41) Squires, R. R.; Cramer, C. J. *J. Phys. Chem. A* **1998**, *102*, 9072.
(42) Energies of OITB in *p*-benzyne can be estimated via a singlet–triplet energy gap (about 3.8 kcal). The difference in singlet/triplet geometries gives, at the same time, indirect information about orbitals involved into OITB. Another estimate of the OITB energy is provided by biradical stabilization energies (BSEs). The upper bound for the BSE energy in *p*-benzyne is about 5 kcal/mol (Davico, G. E.; Bierbaum, V. M.; DePuy, C. H.; Ellison, G. B.; Squires, R. R. *J. Am. Chem. Soc.* **1995**, *117*, 2590). An indirect but fast and quite accurate approach which requires proper calibration is based on analysis of ¹H isotropic hyperfine splitting in aryl radicals as discussed in: Cramer, C. J.; Debbert, S. *Chem. Phys. Lett.* **1998**, *287*, 320.

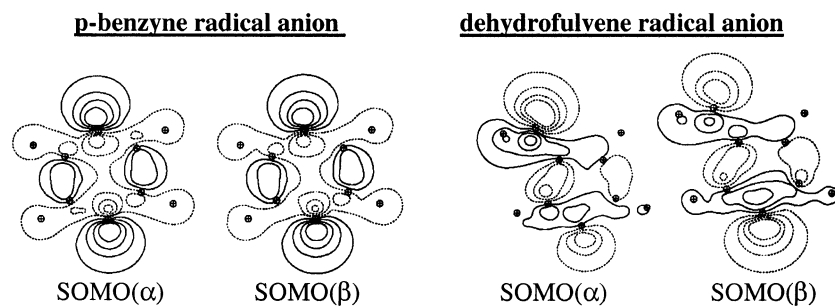


Figure 11. Singly occupied MOs (SOMOs) for the products of radical-anionic cyclizations.

Table 3. Biradical (BSE) and Radical-Anion (RAE) Stabilization Energies (kcal mol⁻¹) of the Products of Thermal Activation

Equation	Method	ΔE_1^a	ΔE_2^b
	B3LYP/6-31G** BLYP/6-31G** BLYP/6-31+G*	1.1 2.4 1.7	1.3 2.6 1.8
	B3LYP/6-31G** BLYP/6-31G** BLYP/6-31+G*	9.1; 6.6^c 14.8; 11.2 13.5; 9.8	7.6 10.6 9.9
	B3LYP/6-31G** BLYP/6-31G** BLYP/6-31+G*	3.6 6.3 5.5	3.5 6.2 5.3
	B3LYP/6-31G** BLYP/6-31G** BLYP/6-31+G*	14.5; 10.9 20.1; 15.7 19.5; 14.1	9.9 15.4 14.8
	B3LYP/6-31G** BLYP/6-31G** BLYP/6-31+G*	12.6; 8.9 17.3; 12.3 16.5; 11.7	8.1 14.2 13.6

^a Stabilization energies for the products derived from the parent enediyne **3**. ^b Stabilization energies for the products derived from benzannelated enediyne **6**. ^c Values in boldface are computed at the SCF-PCM level with acetonitrile as a solvent.

BSEs in fulvene diradicals where the radical centers are anti-periplanar are noticeably increased compared to those in *p*-benzyne, where the radical orbitals are synperiplanar (Table 3).

We found that radical-anion stabilization energies (RASE) for the products of both radical-anionic cyclizations are significantly larger than BSEs for the biradicals produced in the corresponding thermal reactions (Table 6). Increased RASEs significantly contribute to the greater exothermicity of the radical-anionic processes, but a detailed discussion of the origin and consequences of this effect is beyond the scope of the present paper and will be reported in the due course. In brief, this increase can be attributed to the fact that the LUMO of the diradicals, which is populated by the one-electron reduction, corresponds to a symmetric combination of two nonbonding orbitals. This effect and the more spatially diffuse anionic orbitals allow for increased direct through-space interaction of the two radical-anionic centers in *p*-benzyne. The situation is more complicated in the dehydrofulvene radical anion, where the transoid geometry seems to preclude direct through-space overlap.⁴³ Contours of the SOMOs for the two radical anions are given in Figure 11. Our finding of markedly increased

coupling of nonbonding orbitals in σ,σ -radical anions is, to the best of our knowledge, the first report of this phenomenon which may be of general importance for radical-anionic reactions.⁴⁴

4. Substituent Effects on Radical-Anionic Cycloaromatization Reactions. A. Substituent Effects on Kinetics and Thermodynamics. As we discussed above, the low sensitivity of cycloaromatization reactions toward remote substituent effects is a large impediment for efficient control of these reactions. In contrast, both reductive cyclizations are highly sensitive to π -conjugative effects of remote substituents in the aromatic rings. The range of activation energies spans 12 kcal/mol for the C1–C6 cyclization and almost 19 kcal/mol for the C1–C5 cyclization (Figure 12). These differences sharply contrast with the weak substituent effects in analogous thermal processes, where the range of activation energies for the same set of substituents is less than 1 kcal/mol!¹⁷ In contrast to the Bergman cyclization, which is accelerated (weakly) by electron-acceptor substituents in the aromatic ring,^{13,17} the radical-anionic cyclizations are predicted to be accelerated by electron donors. Electron acceptors have the opposite effects, and the activation energy of the *p*-nitro-substituted enediyne is the largest among the computed reaction barriers in Tables 4–6.

(43) Interestingly, the NBO analysis of β -spin-orbitals of the dehydrofulvene radical anion characterizes the in-phase combination of the two nonbonding AOs at C2 and C6 as a σ -bond. This is again consistent with the increased coupling of the two nonbonding orbitals in this radical anion.

(44) For the representative examples of benzyne radical anions, see: Wenthold, P. G.; Hu, J.; Squires, R. R. *J. Am. Chem. Soc.* **1996**, *118*, 11865. Reed, D. R.; Hare, M.; Kass, S. R. *J. Am. Chem. Soc.* **2000**, *122*, 10689.

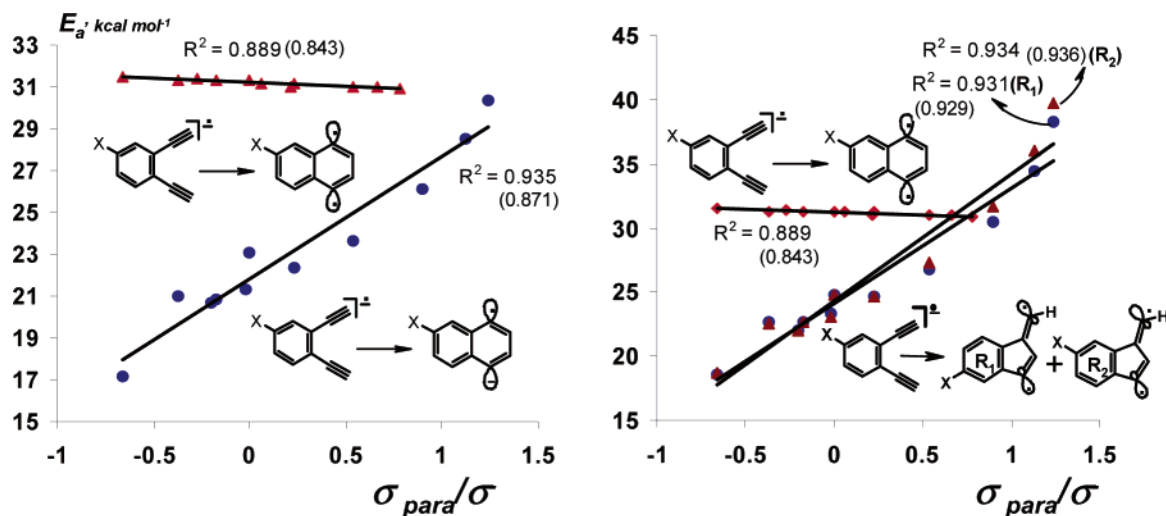


Figure 12. Correlation of UB3LYP(UBLYP)/6-31G** barriers for the radical anionic Bergman and C1–C5 cyclizations of substituted benzannelated enedynes with Hammett constants of remote substituents ($\sigma(-)$ constants were used when available; X = NO₂, CHO, CN, F, Cl, OMe). An analogous correlation for the thermal Bergman cyclization is given for comparison (red triangles).

Table 4. Activation Barriers and Reaction Energies (kcal mol⁻¹) of C1–C6 and C1–C5 Radical-Anionic Cyclizations of Benzannelated Eneidyne Calculated at the UBLYP/6-31+G* Level

R	C1–C6 Cyclization				C1–C5 Cyclization			
	R _{C1C6}	TS _{C1C6}	ΔE [‡] (A)	ΔE _r (A)	R _{C1C5}	TS _{C1C5}	ΔE [‡] (B)	ΔE _r (B)
H	4.451	2.403	18.1	-20.3	3.874	2.401	19.4	-1.8
F, R _a	4.409	2.404	15.9	-22.8	3.857	2.421	17.4	-4.3
F, R _b					3.845	2.390	17.3	-3.9
Cl, R _a	4.405	2.390	16.6	-21.8	3.851	2.390	18.3	-3.1
Cl, R _b					3.849	2.384	18.2	-2.9
CF ₃ , R _a	4.360	2.317	18.5	-17.4	3.805	2.286	21.5	1.2
CF ₃ , R _b					3.832	2.296	22.3	0.8
CN, R _a	4.343	2.280	19.9	-14.9	3.794	2.236	23.5	4.0
CN, R _b					3.819	2.290	24.6	3.5
CHO, R _a	4.308	2.204	22.0	-8.5	3.764	2.144	27.3	9.0
CHO, R _b					3.793	2.198	28.9	10.0
NO ₂ , R _a	4.296	2.151	23.8	-2.3	3.757	2.056	30.9	15.8
NO ₂ , R _b					3.779	2.093	32.1	17.1
NH ₂ , R _a	4.433	2.417	12.1	-23.7	3.869	2.445	13.3	-5.2
NH ₂ , R _b					3.853	2.411	13.5	-4.8
Me, R _a	4.426	2.397	15.1	-22.7	3.860	2.398	16.7	-4.2
Me, R _b					3.862	2.389	16.8	-4.2
OH, R _a	4.411	2.411	15.6	-23.0	3.855	2.446	16.7	-4.9
OH, R _b					3.846	2.399	16.9	-4.2
OMe(syn), R _a	4.325	2.412	15.8	-23.6	3.869	2.434	17.1	-4.1
OMe(syn), R _b					3.854	2.401	16.9	-3.8
OMe(anti), R _a	4.425	2.428	15.0	-23.2	3.866	2.458	15.6	-5.8
OMe(anti), R _b					3.855	2.421	16.0	-5.2

This high sensitivity of both C1–C5 and C1–C6 radical-anionic cyclizations toward conjugative effects of para substituents (below) (Figure 12) is readily explained by the same crossing of in-plane and out-of-plane MOs (Figure 14).⁴⁵ For example, the presence of acceptor substituents strongly stabilizes enediyne radical anions, where the extra electron is delocalized in the *out-of-plane* π -system. After the TS, the extra electron

is transferred to an in-plane MO, the stabilizing effect is considerably weakened, and the total energy of the radical anion is only slightly affected by the substituent. As a result, the activation and reaction energies increase with increasing acceptor ability of the substituents (Figures 12–14). On the other hand, electron donors accelerate the cyclization by destabilizing the reactant radical anion. The possibility to change the reactant

Table 5. Activation and Reaction Energies (kcal mol⁻¹) for the C1–C6 Cyclizations of Benzannelated Eneidyne Radical Anions Computed at the B3LYP/6-31G** (BLYP/6-31G**) Level

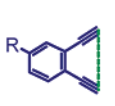
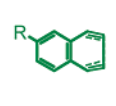
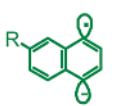
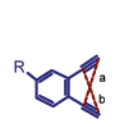
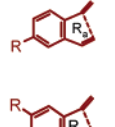
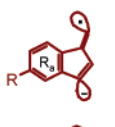
R				
	R _{C1...C6}	TS _{C1...C6}	ΔE [‡]	ΔE _r
H	4.411 (4.457)	2.337 (2.379)	23.1 (19.8)	-18.8 (-18.8)
F	4.369 (4.406)	2.328 (2.381)	21.3 (16.5)	-20.6 (-22.4)
Cl	4.366 (4.399)	2.320 (2.368)	22.4 (17.4)	-19.1 (-21.0)
CF ₃	4.328 (4.364)	2.263 (2.310)	23.6 (18.6)	-15.7 (-17.4)
CN	4.303 (4.337)	2.201 (2.261)	26.1 (20.6)	-11.5 (-13.5)
CHO	4.268 (4.307)	2.127 (2.196)	28.5 (22.5)	-5.2 (-7.4)
NO ₂	4.247 (4.289)	2.070 (2.163)	30.4 (23.6)	0.2 (-2.8)
NH ₂	4.387 (4.428)	2.342 (2.390)	17.2 (12.0)	-21.8 (-23.5)
Me	4.382 (4.414)	2.330 (2.371)	20.8 (16.0)	-20.6 (-21.9)
OH	4.369 (4.407)	2.335 (2.386)	21.0 (16.1)	-21.0 (-22.7)
OMe(<i>sym</i>)	4.386 (4.424)	2.334 (2.383)	21.4 (16.2)	-20.9 (-22.5)
OMe(<i>anti</i>)	4.375 (4.411)	2.345 (2.395)	20.7 (16.0)	-21.2 (-22.9)

Table 6. Activation and Reaction Energies (kcal mol⁻¹) for the C1–C5 Cyclizations of Benzannelated Eneidyne Radical Anions Computed at the B3LYP/6-31G** (BLYP/6-31G**) Level

R				
	R _{C1...C5}	TS _{C1...C5}	ΔE [‡]	ΔE _r
H	3.843 (3.877)	2.378 (2.377)	24.8 (21.5)	0.3 (-0.7)
F (R _a)	3.815 (3.844)	2.403 (2.403)	23.3 (18.4)	-1.3 (-3.9)
F (R _b)	3.815 (3.844)	2.360 (2.368)	23.1 (18.1)	-1.5 (-4.3)
Cl (R _a)	3.818 (3.845)	2.356 (2.360)	24.7 (19.6)	0.4 (-2.4)
Cl (R _b)	3.818 (3.845)	2.356 (2.357)	24.6 (19.3)	0.2 (-2.6)
CF ₃ (R _a)	3.800 (3.830)	2.274 (2.270)	26.8 (21.6)	3.2 (0.5)
CF ₃ (R _b)	3.800 (3.830)	2.308 (2.305)	27.3 (22.3)	3.3 (0.8)
CN (R _a)	3.782 (3.811)	2.201 (2.200)	30.4 (24.6)	7.7 (4.5)
CN (R _b)	3.782 (3.811)	2.259 (2.253)	31.6 (25.9)	7.9 (5.0)
CHO (R _a)	3.760 (3.791)	2.124 (2.119)	34.4 (27.8)	13.5(10.6)
CHO (R _b)	3.760 (3.791)	2.178 (2.166)	36.0 (29.5)	13.4(9.8)
NO ₂ (R _a)	3.741 (3.776)	2.042 (2.059)	38.3 (30.3)	19.2 (14.9)
NO ₂ (R _b)	3.741 (3.776)	2.074 (2.094)	39.7 (31.7)	19.7 (16.0)
NH ₂ (R _a)	3.822 (3.853)	2.430 (2.425)	18.6 (13.5)	-2.8 (-5.3)
NH ₂ (R _b)	3.822 (3.853)	2.386 (2.388)	18.7 (13.4)	-2.8 (-5.6)
Me (R _a)	3.830 (3.855)	2.376 (2.371)	22.7 (18.0)	-1.6 (-4.0)
Me (R _b)	3.830 (3.855)	2.367 (2.364)	22.7 (18.0)	-1.5 (-4.0)
OH (R _a)	3.816 (3.846)	2.373 (2.425)	22.6 (17.6)	-1.8 (-4.5)
OH (R _b)	3.816 (3.846)	2.426 (2.380)	22.5 (17.6)	-2.3 (-5.0)
OMe(R _a , <i>sym</i>)	3.822 (3.851)	2.410 (2.409)	23.2 (18.4)	-1.2 (-3.9)
OMe(R _b , <i>anti</i>)	3.821 (3.850)	2.435 (2.430)	22.0 (17.3)	-2.8 (-5.4)
OMe(R _a , <i>sym</i>)	3.822 (3.851)	2.369 (2.374)	23.0 (18.1)	-1.3 (-3.8)
OMe(R _b , <i>anti</i>)	3.821 (3.850)	2.390 (2.394)	22.2 (17.2)	-2.4 (-5.0)

energy while keeping absolute energies of the transition state and the product almost unchanged allows for substituent controlover reactivity, which is unprecedented for cycloaromatization reactions.

The excellent correlation of the ΔE_a and ΔE_r values with the Hammett σ(–)_p substituent constants confirms that observed effects result from π-conjugative effects of substituents (Figure 12). Finally, in agreement with the MO crossing model⁴⁶ in Figure 14 and with the Hammond postulate,⁴⁷ there is a good correlation between the incipient C1–C6 (or C1–C5) distances in the transition states for the corresponding cyclizations and activation and reaction energies for the cyclizations, as illustrated in Figure 15. As expected, more exothermic reactions have earlier transition states.

Despite the wide range of reaction energies for the cyclizations of substituted eneidyne, the difference in reaction energies (but not in the activation energies) between the C1–C5 and C1–C6 pathways stays approximately the same (ca. 18 kcal/mol) independent of the substituents, which indicates that this difference may be an intrinsic property of these reactions.

The observation that cycloaromatization reactions can be made sensitive to benzannelation and remote substituent effects by temporary population of an out-of-plane MO (the LUMO) may have consequences beyond radical-anionic cyclizations. According to our preliminary results, photochemical population of the eneidyne LUMO⁴⁸ also renders both the Bergman and the C1–C5 cyclizations sensitive to the benzannelation effect (Table 1). These studies will be reported in due course.

B. Geometries. Geometry changes for two benzannelated eneidyne with para substituents of opposite polarity are given in Figure 16 (see also Figure 5 for the geometries of unsubstituted benzannelated radical-anion and corresponding reaction intermediates). Differences in geometries of reaction intermediates for the cyclizations of nitro and amino eneidyne in Figure 16 illustrate how remote substituents influence the distribution of electron density along the whole reaction path. Changes in the bond lengths are consistent with the delocalization of electron density from the para “acetylenyl” π-system to the nitro group in the first case but increased *localization* of the negative charge in the meta acetylenyl moiety in the second case.

More importantly, transition states for the cyclizations of donor-substituted eneidyne are significantly earlier than for eneidyne with electron acceptor substitution. This is obvious upon inspection of incipient C1–C6 (or C1–C5) bond lengths and C1–C2–C3 angles in the corresponding transition states (Figures 15 and 16).

C. Substituent Effects on Reduction Potentials of Eneidyne. Although introduction of electron donor substituents facilitates the cyclization due to reactant destabilization, the tradeoff is in the increase in eneidyne reduction potentials, which makes generation of the radical anions more difficult. Therefore, we have estimated reduction potentials of substituted eneidyne relative to 1,2-diethynyl benzene **6** using the isodesmic equation in Scheme 5. Interestingly, there are two substituents (F and Cl) that are reduced more readily than eneidyne **6** but also are

(45) We have used the hybrid DFT method B3LYP to gauge substituent effects on the radical-anionic cyclizations. This method overestimates the activation energy for the cyclization but is also capable of reproducing general trends in reactivity upon one-electron reduction. We are interested in relative trends in reactivity, and somewhat lesser accuracy in description of the cyclization process per se is compensated by an overall better description of substituent effects by the more general hybrid DFT method.

(46) The relation to the Pross–Shaik curve crossing model is also obvious: Pross, A.; Shaik, S. S. *Acc. Chem. Res.* **1983**, *16*, 363.

(47) Hammond, G. S. *J. Am. Chem. Soc.*, **1955**, *77*, 334.

(48) In the parent eneidyne the lowest energy excitation is essentially a HOMO–LUMO transition.

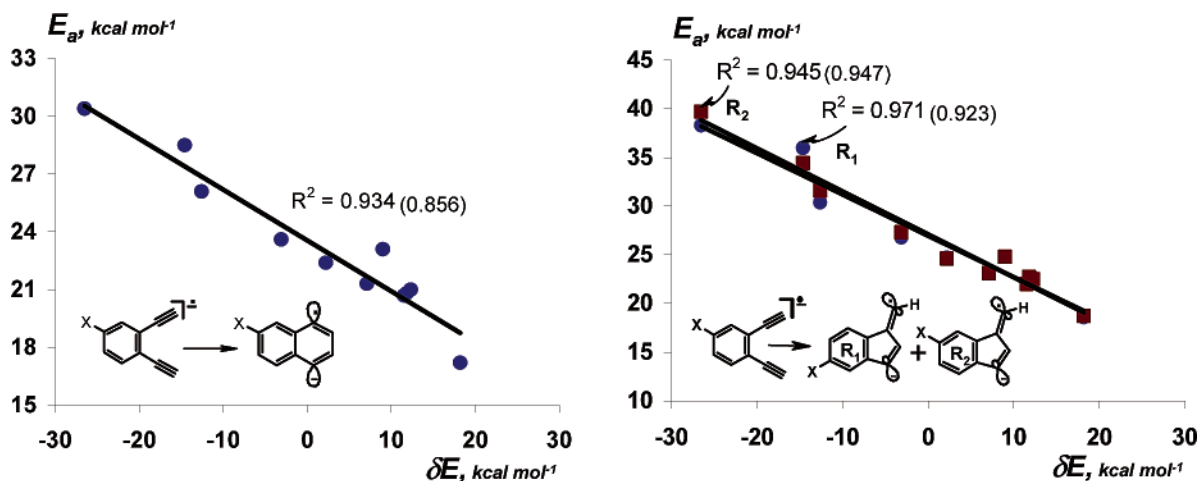


Figure 13. Correlation of the UB3LYP(UBLYP)/6-31G** barriers for the radical anionic cyclizations of various benzannulated eneidyne with “substituent destabilization energy” (i.e. the energy difference between the neutral and radical anion eneidyne).

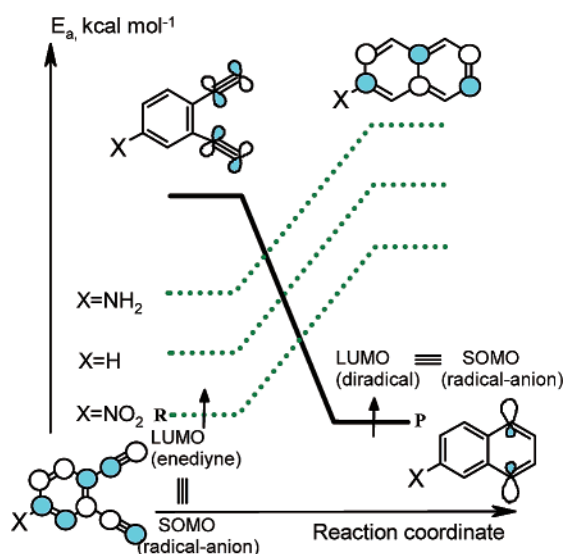


Figure 14. Substituent effects on the crossing between *in-plane* and *out-of-plane* MOs of the eneidyne moiety along the reaction coordinate of radical-anionic Bergman cyclization.

predicted to increase the cyclization rate. Still, for the majority of accelerating substituents, a price for the increased reactivity has to be paid during the reduction step (NH₂, Me, OH, OMe). The reactant destabilization of such eneidyne with donor substituents is almost completely converted into increased reaction exothermicity for Me-, OH-, and OMe-substituted *p*-benzyne radical anions but not for the NH₂ substituent, where the product is still destabilized considerably. On the other hand, electron acceptors should noticeably facilitate the eneidyne reduction step but, due to loss of the conjugation with the anionic center during the cyclization process, this stabilization is drastically diminished in the products and, as a result, the cyclizations are endothermic. The larger part of residual stabilization in CN-, CHO-, and NO₂-substituted *p*-benzyne radical anions seems to be a predominantly field or inductive effect rather than a π -acceptor effect, as illustrated by comparison with CF₃- and Cl-substituted eneidyne.⁴⁹

5. Kinetic and Thermodynamic Control and Competition between the C1–C5 and C1–C6 Pathways. Although the Bergman cyclization has been known for a long time, the C1–C5 pathway is quite unusual. In addition to being mechanisti-

cally interesting, it may also complement the C1–C6 (Bergman) pathway in future synthetic applications.⁵⁰ Therefore, it is important to determine what controls regioselectivity of eneidyne cyclizations: i.e., competition between C1–C5 and C1–C6 cyclizations of eneidyne. Both radical-anionic cyclizations of 1,2-diethynylbenzene (**6**) are predicted to occur under ambient conditions. Although the activation energies for C1–C5 and C1–C6 radical anionic cyclizations are quite close (19.4 vs 18.1 kcal/mol at the B3LYP/6-31G** level of theory), the 6-*endo* cyclization path clearly should dominate in the case of eneidyne *with* terminal substituents, the competition between these two possible pathways is likely to be a result of a rather subtle balance between steric and electronic effects. As has been pointed earlier by Schreiner, terminal substituents should generally favor fulvene formation, especially when such substituents are bulky.²⁷ The higher exothermicity of the C1–C6 cyclization is likely to offset the steric destabilization up to a certain threshold, after which a switch to a C1–C5 cyclization should occur. The computational results in Figure 4 also suggest that even when the C1–C5 mode is kinetically favored, the highly exothermic anionic C1–C6 cyclization still may be observed under thermodynamic control conditions (equilibration of reaction intermediates).

Finally, one may also note that electron acceptors have a considerably larger decelerating effect on the radical-anionic C1–C5 cyclization than on the radical-anionic Bergman reaction (Table 3). Therefore, an appropriate choice of remote substituents is also a good way to fine-tune the regioselectivity of these cyclizations.

Conclusion

In summary, temporary population of the eneidyne lowest

(49) The presence of an electronegative substituent should also increase the weight of the electronic configuration, where the lowest unoccupied out-of-plane MO (LUMO+1) is populated because the energy gap between in-plane and out-of-plane MOs in the product decreases. Although DFT methods are monoconfigurational, they might be able to recover a part of correlation energy and indirectly reproduce these multiconfigurational effects.

(50) Note, however, that eneidyne can be transformed into fulvenes by several other routes, including the diradical pathway suggested by Schreiner in ref 27, additions of radical (Konig, B.; Pitsch, W.; Klein, M.; Vasold, R.; Prall, M. Schreiner, P. *J. Org. Chem.* **2001**, *66*, 1742) and electrophilic and nucleophilic¹⁹ species to eneidyne, and cyclizations of eneidyne radical cations.^{21a,b}

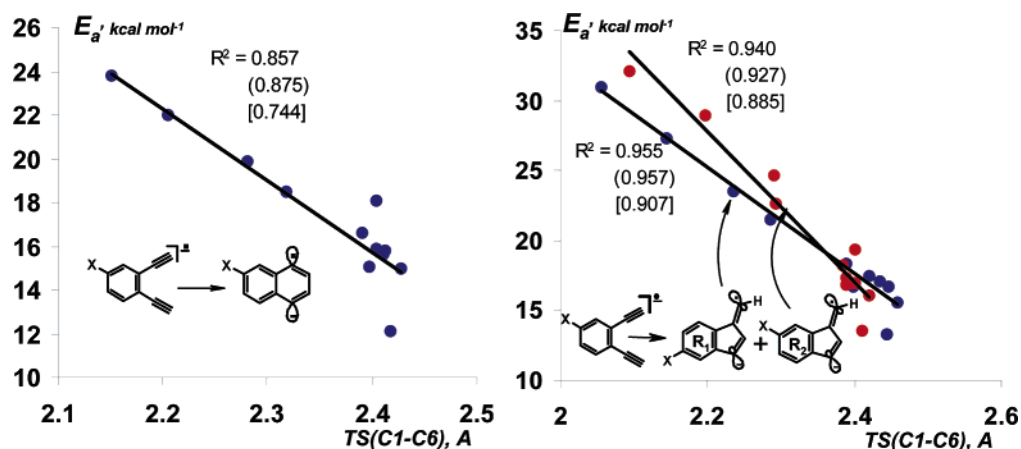


Figure 15. Correlation of activation barriers of the radical anionic cyclizations of benzannulated enediyne with the incipient bond lengths (C1...C6/C1...C5) at the TS calculated at the UBLYP/6-31+G* (UB3LYP/6-31G**) [UBLYP/6-31G**] levels.

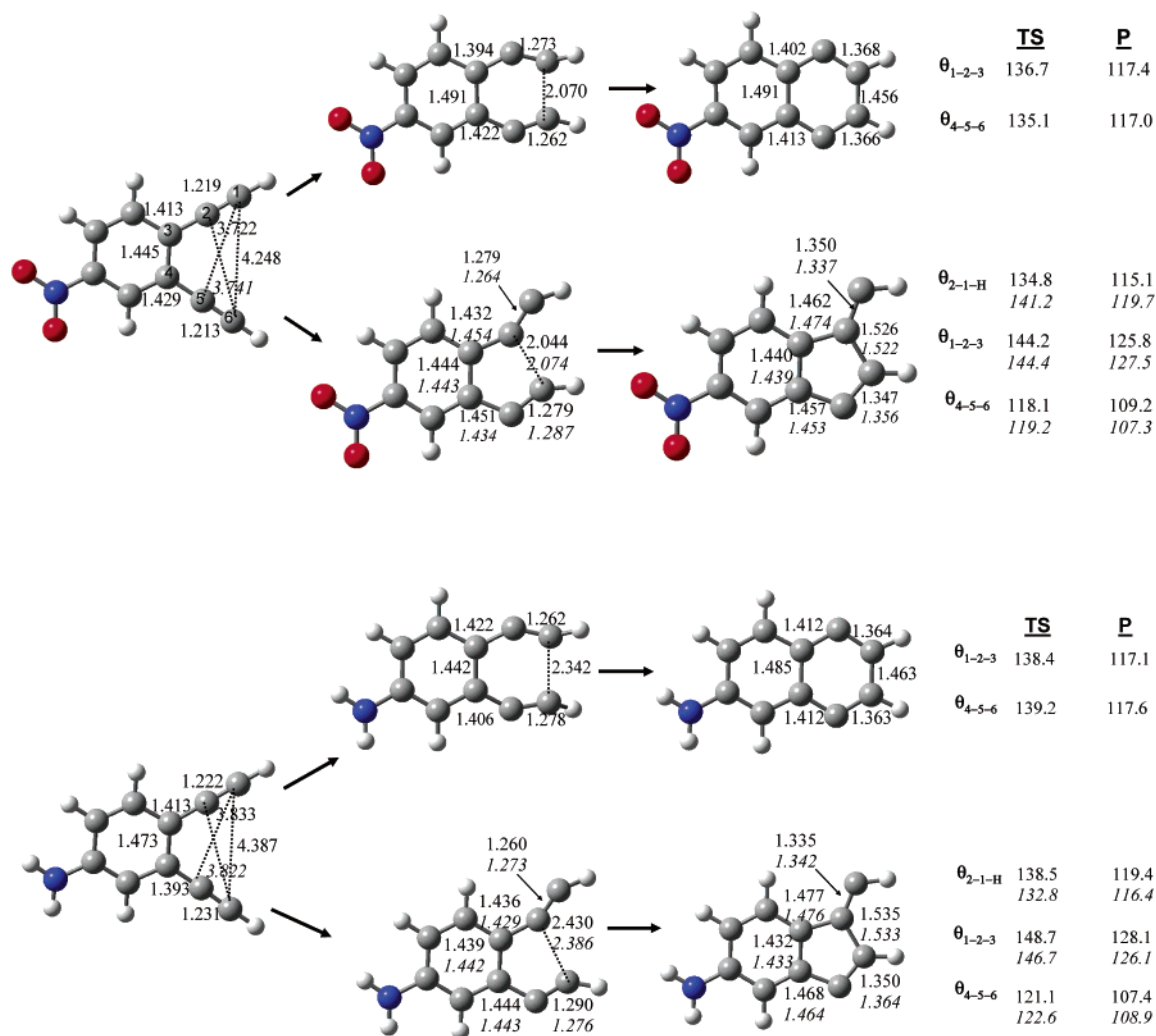
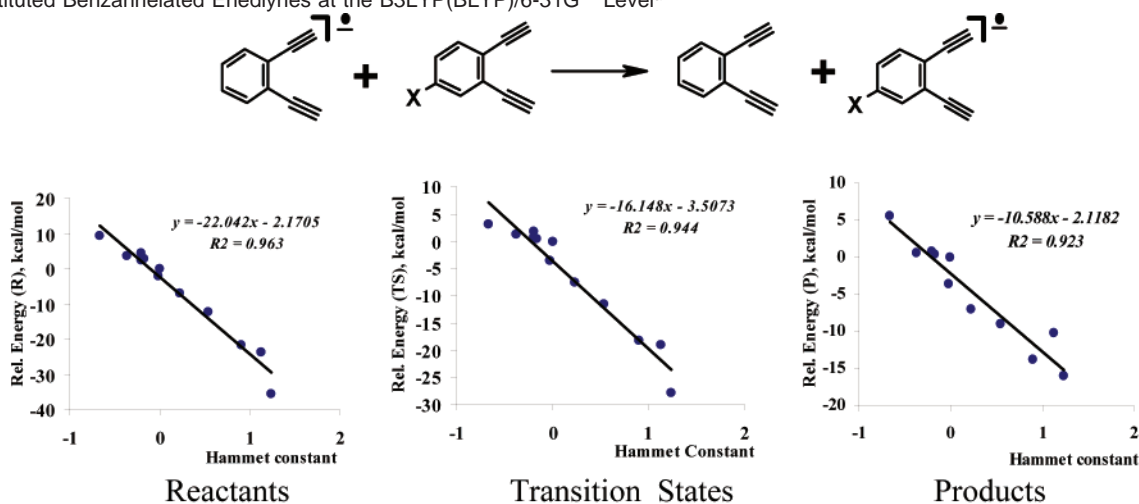


Figure 16. B3LYP/6-31G** geometries of reactants, TSs, and products from the radical-anionic C1–C6 and C1–C5 cyclizations of *p*-nitro- and *p*-amino-substituted benzannulated enediyne (values in italics correspond to formation of the regioisomer where the substituent is meta to the exocyclic double bond of the fulvene moiety).

out-of-plane MO through one-electron reduction renders both C1–C6 and C1–C5 cyclizations of enediyne highly sensitive to benzannulation and to remote substituent effects in the annealed aromatic moieties. This sensitivity is a result of an interesting dynamic interplay between aromaticity and antiaromaticity along the reaction path, which is collectively illustrated

by structural, energetic, and magnetic criteria. An important feature of radical-anionic cyclizations of benzannulated enediyne is that the reactant radical anions are destabilized by loss of aromaticity which occurs upon one-electron reduction. As the reaction proceeds, crossing of *in-plane* and *out-of-plane* MOs in the vicinity of the TS restores aromaticity. As a result, the

Scheme 5. Relative Stabilities of Reactants, Transition States, and Products of Radical-Anionic C1–C6 Cyclizations of Substituted and Unsubstituted Benzannellated Eneidyne at the B3LYP(BLYP)/6-31G** Level^a

R	F	Cl	CF ₃	CN	CHO	NO ₂	NH ₂	Me	OH	OMe _{syn}	OMe _{anti}
Reactant	-1.9 (0.1)	-6.8 (-5.0)	-12.1 (-10.4)	-21.6 (-19.4)	-23.8 (-22.0)	-35.5 (-32.5)	9.2 (11.2)	2.8 (4.2)	3.6 (5.2)	2.5 (4.4)	4.3 (6.1)
TS (C1-C6)	-3.6 (-3.2)	-7.5 (-7.3)	-11.6 (-11.4)	-18.3 (-18.3)	-19.1 (-19.2)	-27.9 (-28.3)	3.0 (3.1)	0.3 (0.3)	1.1 (1.5)	0.8 (1.2)	1.7 (1.8)
Product (C1-C6)	-3.6 (-3.5)	-7.0 (-7.0)	-9.0 (-8.9)	-13.8 (-13.8)	-10.1 (-10.0)	-15.9 (-15.8)	5.6 (6.0)	0.5 (0.7)	0.7 (1.0)	0.7 (0.9)	0.9 (1.2)

^a The isodesmic reaction used to calculate the relative stabilities is illustrated for the reactants (below). Isodesmic reactions for the transition states and the products are analogous.

efficiency of the C1–C6 (the Bergman) cyclization increases dramatically and even the exotic C1–C5 pathway becomes viable. We suggest that this new class of cycloaromatization reactions be appropriately named *cycloaromatization reactions*.

Although the reactant energy is highly sensitive to π -conjugative effects of substituents, once the crossing point (the TS) is passed, the substituent effects on the *absolute* energy of the TS and the product are less important. Changing the reactant energy on keeping the TS and product energies relatively constant allows control over the activation and reaction energies to an extent which is unprecedented for cycloaromatization reactions.

Our computational results also suggest possible ways to control regioselectivity of the ring closure and steer the reaction to either a C1–C6 or a C1–C5 pathway. While (dependent on substitution) the C1–C5 pathways may be favored under kinetic control conditions (rapid quenching of the radical anion), the highly exothermic C1–C6 pathways should be favored under thermodynamic control (slow equilibration of reaction intermediates).

Finally, this study outlines a new approach to a variety of facile, easily triggered, and efficiently controlled cycloaromatization processes. Taking into account the vast body of practical applications of thermal cycloaromatization reactions, we foresee a fast development of their radical-anionic cousins soon.

Acknowledgment. I.V.A. is grateful to Florida State University for a First Year Assistant Professor Award, to the donors of the Petroleum Research Fund, administered by the American Chemical Society, for partial support of this research, and to the 3M company for an Untenured Faculty Award.

Supporting Information Available: The activation and reaction energies of the corresponding diradical cyclizations calculated at UB3LYP and UBLYP levels, the plots from UBLYP data, the contours of FMOs as well as the major π -orbital interactions from NBO analysis, and the Cartesian coordinates of all optimized geometries with total energy (au) (PDF). This material is available free of charge via the Internet at <http://pubs.acs.org>.

JA029664U